Addis Ababa University

The School of Graduate Studies

College of Natural and Computational Sciences

School of Earth Sciences

SEISMIC REFLECTION STUDIES OF SOUTH OMO BASIN, SOUTH WESTERN ETHIOPIA

A Thesis

Submitted to

The School of Graduate Studies
of Addis Ababa University

In partial fulfillment of the requirements for the Degree of
Master of Science in Applied Geophysics

by
Tefera Alemu

June, 2017

Addis Ababa University
School of Graduate Studies
College of Natural and Computational Sciences

SEISMIC REFLECTION STUDIES OF SOUTH OMO BASIN, SOUTH WESTERN ETHIOPIA

By
Tefera Alemu Zemedagegnehu
School of Earth Sciences

Approved by board of examiners:-

1. Dr. Balemwal Atnafu	Signature _____
(Head, School of Earth sciences)	Date _____
2. Professor Tilahun Mammo	Signature _____
(Advisor)	Date _____
3. Dr Atalay Ayele	Signature _____
(Examiner)	Date _____
4. Professor Tigistu Haile	Signature _____
(Examiner)	Date _____

Abstract

Forty one Seismic lines have been acquired by Tullow oil in 2010-2011 in South Omo basin. Of these twelve selected seismic lines are processed and interpreted in this study. The selections of the seismic lines are based on the results of previous gravity analysis and borehole information from Sabisa-1. Nine of the seismic lines are E-W oriented and the rest have N-S orientations. During data acquisition, both Vibrator and explosive sources were utilized.

The data processing was carried out using Vista 2D/3D version 12.0 seismic processing software. The various layers as well as the structures affecting the basin are interpreted with OpendTect software version 6.0.5.

The results show a westward dipping half-graben sedimentary basin bounded by a north-south striking major fault. Deposition of thick sediments was observed in the southern part of the basin near Lake Turkana as well as in the northern part of the basin around seismic Line SO-20. The sediments thin out towards the east of the Omo River. The study also identifies a likely hydrocarbon prospective area near Line SO-20.

The result of the work is believed to serve as an additional guide for further hydrocarbon exploration program over the area.

Acknowledgments

Above all I would first and foremost like to praise the Almighty God for being on my side throughout my entire life and for encompassing me with His endless love.

Next my deepest gratitude goes to different individuals, who had contributed a lot for the success of this thesis. First I am deeply indebted to my advisor Professor Tilahun Mammo for making his time and knowledge available, for the valuable comments, guides and for continuously following up the whole progress of this work. I have benefited immensely from the assistance, advice and cooperation throughout my study.

Likewise, my Mother, brothers and sisters deserve special thanks beyond what words can express. When they should be getting my assistance, they, instead, have shared my pains and helped me to make my dream come true. I can never forget their unreserved moral support, understanding and concern.

My heartfelt and deepest thanks go to my wife Sisay Woldehanna and my children Samson and Eyuel who were always by my side throughout the ups and downs of my life. I would like to express my special thanks to Petros Abebe, Manager of Tullow oil Ethiopia, and to Alemayehu Berhie for their various assistances. I would like also to convey my special thanks to Sisay Alemayehu, Mebatsion Shawol, Workineh Gebru, Bisrat Kebede, Tagel Assefa and Tadele Nigussu for their encouragement and assistance throughout my academic work.

Last but not least, Dr. Ketsela Tadesse Director of Petroleum Licensing and Administration Directorate must be thanked for his genuine understanding and encouragement throughout my academic work. I owe special thanks to the Ministry of Mines, Petroleum and Natural Gas for sponsoring my studies and for providing raw data for my research.

Finally, I thank the entire staff of the School of Earth Sciences and IGSSA for their conducive environment they created for me to complete my study and the various assistance extended to me.

Table of contents

List of figures

Acronyms

2D	Two Dimension
AGC	Automatic Gain Control
CDP	Common Depth Point
CMP	Common Mid-Point
CVS	Constant Velocity Spectrum
EARS	East African Rift System
EIGS	Ethiopian Institute of Geological Survey
FDRE	Federal Democratic Republic of Ethiopia
FFT	Fast Fourier Transform
FTG	Full Tensor Gradient
GR	Gamma Ray
IFFT	Inverse Fast Fourier Transform
JSA	Joint Study Agreement
Km	Kilometer
MER	Main Ethiopian Rift
MT	Magneto Telluric
NMO	Normal Move Out
POD	Petroleum Operation Department
PPSA	Petroleum Production Sharing Agreement
RMS	Root Mean Square
SEGD	Society of Exploration Geophysics version D
SEGY	Society of Exploration Geophysics version Y
SMT	Seismic Micro Technology
SO	South Omo
SP	Spontaneous Potential
TVSB	Time Variant Spectral Balancing

CHAPTER ONE

1. INTRODUCTION

There are six Sedimentary basins found Ethiopia. These are Ogaden basin, Abay basin, Gambella basin, Mekele basin, Metema basin and Main Rift valley of Ethiopia (MRE) basin. Exploration of Oil and Gas has started in Ethiopia since 1970's. The first discovery was in Ogaden basin in 1970's by American Company known Tenneco Oil Plc. Later on in the 1980's Soviet Petroleum Exploration Expedition have acquired several 2D seismic and have drilled several wells in the Ogaden basin.
Many Exploration companies have been participated to search oil and gas in the 1990's and 2000's (Hunt oil, Maxus, and PETRONAS). Still there are exploration companies working in Ethiopia to find oil and gas.

The East African Rift System (EARS) has attracted the academia and business companies to have interest in exploration for hydrocarbon and geothermal resources. It has become a focus of research areas to expand the understanding of the subsurface structures, stratigraphy and petrology of the rift (Feibel, 2011). The discovery of oil in Albert basin (Uganda) in 2006 has advanced the interest of Tullow Oil and other exploration companies (Annual report of Tullow Oil plc, 2006). They extended their mission to central and Northern Kenya. Tullow further extend its reach and farm in to the South Omo block exploration license agreement that had been signed by White Nile Limited with Ministry of Mines in 2008 (PPSA, 2008). This research was carried out in South Omo basin located in the southwestern tip of Ethiopia.

South Omo basin is a N-S trending half- graben system. It is situated within the topographic depression that separates the Ethiopian dome from the Kenyan dome. It is also located between the NW-SE trending portfolio Muglad-Melut rift basins of the South Sudan and similarly trending highly prospective Anza basin of Kenya (Figure 1-1).

According to Chorowicz (2005), the half-graben basins that lie in the Omo-Turkana zone between the Ethiopian and Kenyan rifts are of smaller dimensions, with no uplifted shoulders. This lack of uplifted shoulders indicates that the basins are not associated to ascending asthenospheric bodies. According to a study carried out by Beicip Franlab (Beicip Franlab, 1998) the Tertiary succession of the basins are mainly volcanic with fluvial to lacustrine intercalations. It is estimated that more than 3.5 km of sediments fill the South Omo basin located in the area.

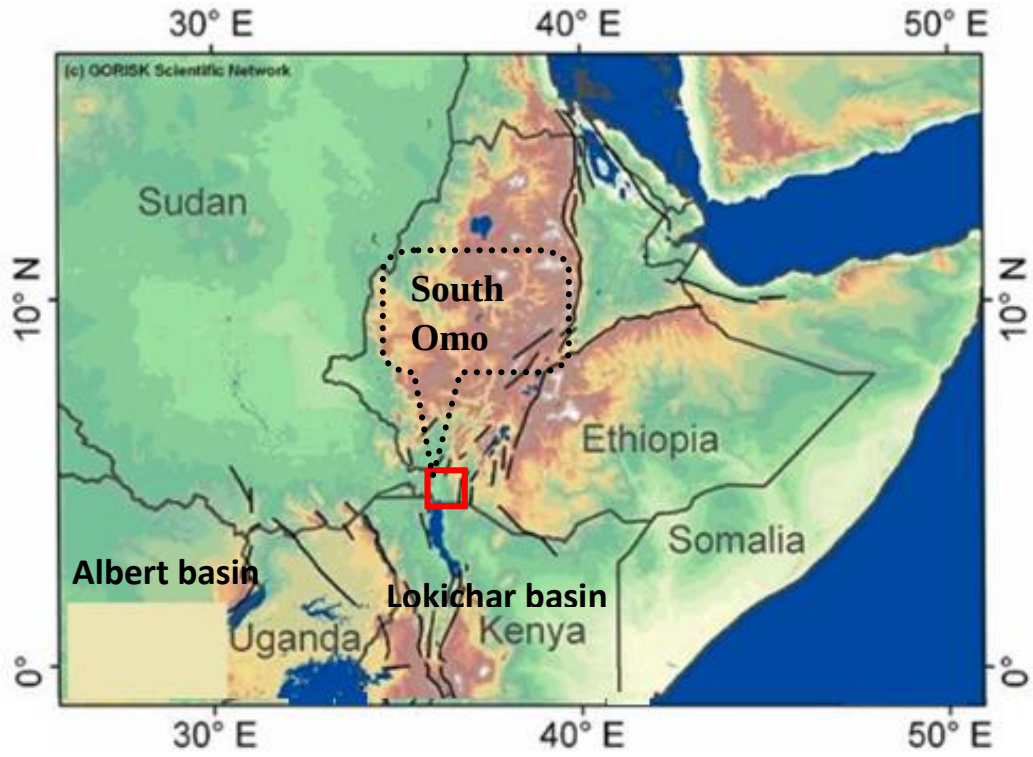

Figure 1-1: Regional structural setting of the study area (after Georisk Scientific Network, 2014).

1.1. Statement of the problem

Since the study area is within the East African Rift system, hydrocarbon occurrence and distribution in the rift is largely a product of stratigraphic succession in the syn- and post-rift phases of the basin evolution. South Omo basin involves two evolution

periods: the formation of Anza graben during Mesozoic period and the formation of East African Rift during, Cenozoic period (Morley et al., 1999).

The interest of oil companies to explore South Omo basin was enhanced after the discoveries of oil in Albert Graben in Uganda and oil discoveries in Lokichar basin of Kenya in the rift. One profile of geophysical survey (gravity and magnetic) along the road from Turmi to Omorate was done by Ministry of Mines, Petroleum Operation Department (POD) in South Omo basin (Ermyas Nigusse et al., 2002). Magnetotelluric (MT) survey was conducted by White Nile Ltd in the year 2007; (Hautot et al., 2007). In 2007 White Nile has acquired airborne gravity and magnetic as well over the area (JSA, 2007). The gravity analysis done by Tilahun Mammo (2012) and the result of MT by Hautot et al., (2007) suggest that about 4 km thick sediments exist in the basin (Figure 1-2).

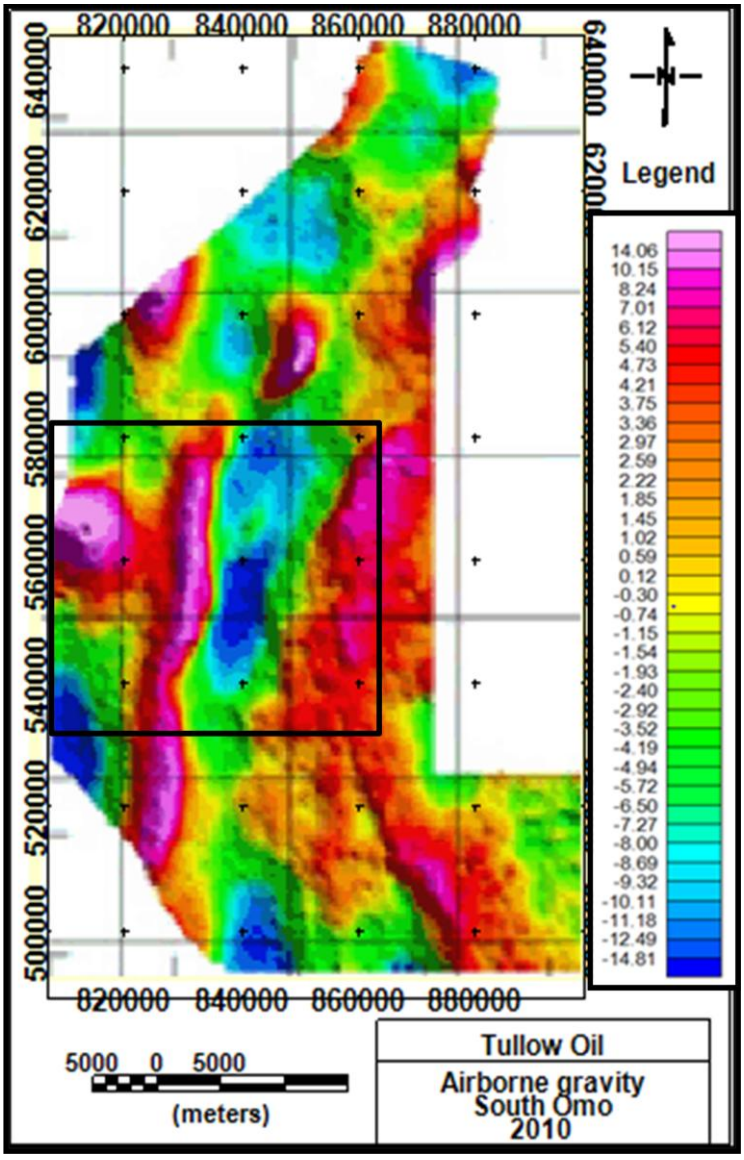

a) Airborne gravity (after Tullow Oil, 2010).

(b)

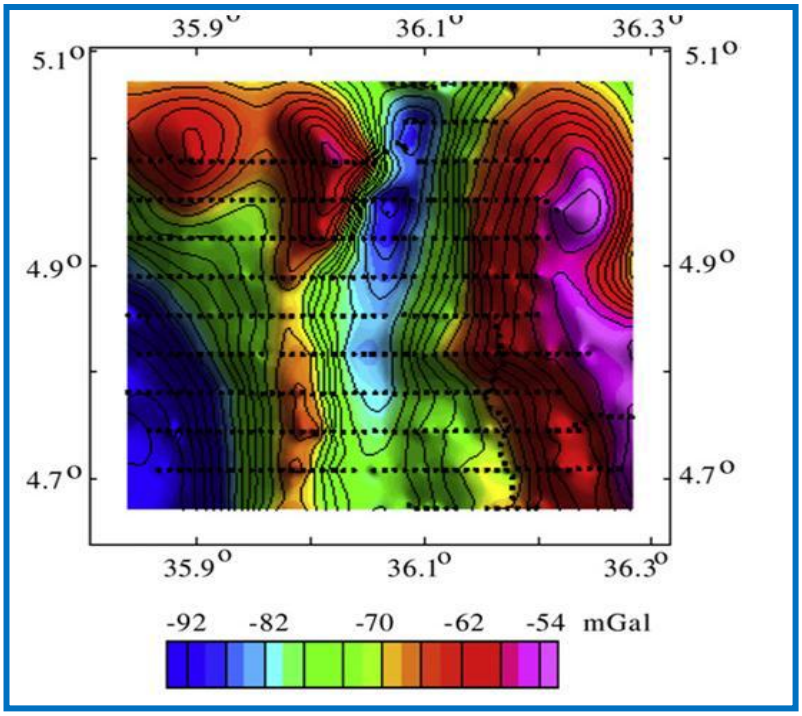

Figure 1-2: Bouguer gravity anomalies of Omo basin:a) airborne gravity (after Tullow oil, 2010) and b) ground gravity (after Tilahun Mammo, 2012).

In 2010 Tullow Oil Company, Africa oil and Marathon oil have attained to accomplish the agreement signed by White Nile. Therefore, Tullow oil, the operator, has acquired airborne gravity, 41 lines of 1002 km 2D seismic data and has drilled two wells in this basin.

Hence, the purpose of this research is to come up with the structures of this basin with one of the geophysical method i.e. seismic method. In addition to this, it is believed the work would help to recommend prospects for oil and gas in the region.

1.2. The study area

1.2.1. Location

South Omo Basin is located in the south western Ethiopia, South Omo Zone, near Omorate Town. It is about 860 Km from Addis Ababa to the border of South Sudan

and Northern Kenya (Figure 1-3). It is located between latitudes 4°30′ - 5°30′ North and Longitudes 35°30′ - 36°30′ East.

The study area can be reached from Addis Ababa by asphalt road via Arbaminch, Konso, Weyto to Keyafer and then by an all weather track via Turmi to Omorate town. There is also one air strip for light airplanes ten kilometer east of Omorate town.

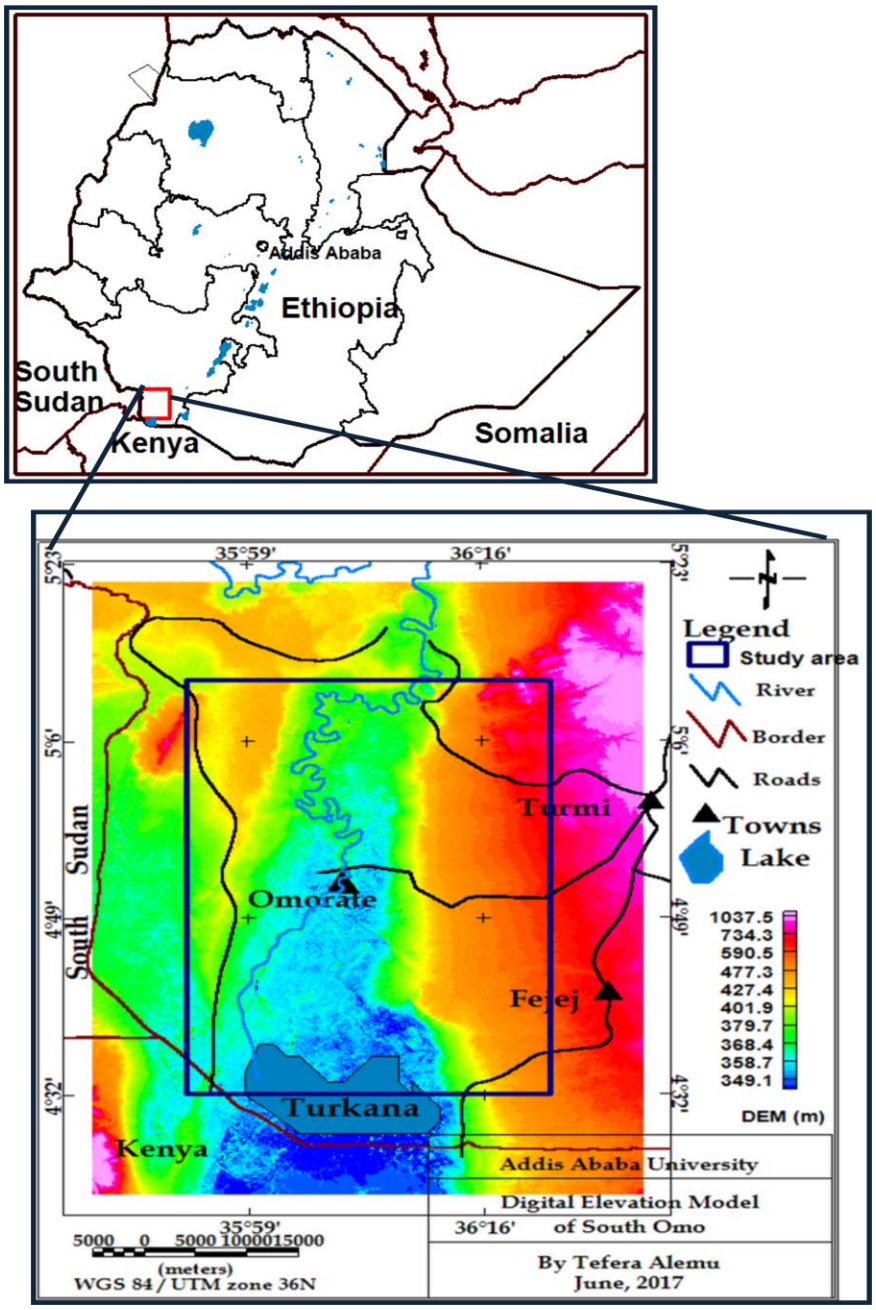

Figure 1-3: Location of the study area.

1.2.2. Physiography, Climate and Vegetation

According to Davidson (1983), physiographic division of South Omo basin categorized under Low lands and rift valley basins. It lies in the drainage of the Omo River which enters Lake Turkana. Lake Turkana is the lowest part of the basin and elevation increases towards both the east and north direction. The study area can be divided in to four types of features: hilly area in the eastern part, flat area with bush in the middle, dense forest around Omo river and Archeological area in west of the Omo river. The plain of South Omo basin has elevations ranging between 400-500m above mean sea level.

The climate of South Omo basin varies from a hot arid climate in the southern part of the floodplain to a tropical sub humid in the highlands that include the extreme north and north western part of basin. It experiences a semiarid or tropical wet and dry climate with two rainy seasons. The daily low temperatures varied from 15^{o}C to 25^{o}C and high temperatures were from 30^{o}C to 40^{o}C (Tullow oil, 2012). The mean annual rainfall in the study area falls in the range of 300-700 mm per annum (Abdella Kemal, 2013). The predominant wet and dry seasons are as follows:

- Dry season (December to March)
- Wet season (April to November)

The bank of Omo River is highly vegetated whereas to eastern and western part of the Omo River have less vegetation with open grasslands.

1.3. Justification and significance of the research

The Northern Kenya rift and Albert rift are part of East African Rift System. There is discovery of oil in loperot-1 in 1992 and Ngamia-1 in 2012 in the Northern rift of Kenya (NOCK, 2012). In the Albert graben, there was also a major discovery of oil in 2006 (Annual report of Tullow Oil Plc, 2006).

The South Omo basin is an extension of this tertiary rift system. It has similar geological and structural features with those basins in the rift. Through this research, re-interpretation of 2D seismic data provides relevant structural and geological information. The research result will help and stimulate companies to have concern in the area. The discovery of oil and gas will also be of great importance to the economy of the country.

1.4. Objectives of the Study

1.4.1. General Objective

The main objective of this study is to determine the subsurface structures and possible hydrocarbon prospective structure within the South Omo basin in the area where seismic reflection data are available from earlier survey.

1.4.2. Specific Objectives

- To map the sequence of rock types and basement highs in the basin through re-interpretation of the seismic sections using well log data.
- To determine the structures those occur within the basin and their characteristics.
- To suggest the occurrence of possible hydrocarbon prospective structure.

1.5. Methodology

To carry out the research work, the data acquired by Tullow Oil Company with Africa Oil and Marathon oil in 2010 and 2011 was used. A total of twelve seismic lines are processed and interpreted. The survey parameters and acquisition method are given below.

The acquisition of the 2D seismic used the following parameters during project operation by its contractor BGP Geoservices plc (Tullow Oil, 2012).

Data Transformation to WGS-84

Dx=0m Dy=0m Dz=0m

WGS-84 Spheroid

Semi-major Axis

Inverse filtering

Unit's international meters

Reference Ellipsoid

- Current Geiod Model: EGM96
- Vertical Datum: Ellipsoid height
- Horizontal Datum: WGS-84
- Ellipsoid : WGS-84
- Semi Major axis (6,378,137.00)
- Inverse of flattening 1/f:1/298.257223563

Projection

- Projection: Universal Transverse Mercator (UTM)
- Vertical Datum: Mean Sea Level
- Horizontal Datum: WGS-84
- Ellipsoid: WGS-84
- Inverse of flattening 1/f: 1/298.257223563
- Grid Name: Zone 36N
- Central Meridian : 33^{o}E
- Latitude of Origin: 0^{o}N
- Longitude of origin: Greenwich
- False Easting: 500,000.00m
- False Northing: 0.00m
- Scale factor at Origin: 0.9996
- Units of Measurements: International Meters

Spread Geometry

Normal 2D spread: 160-0-160

Channels: 320

Nominal Full Fold: 80

Min. Offset: 12.5m

Max. Offset: 3987.5m

Receiver Interval: 25m

Source Interval: 50m

Receiver

Geophone type: 20-DX

Geophone array: Linear

Geophones per array:12

Array length: 25m

Geophone space: 2.08m

Receiver Interval: 25m

Receiver array: Linear

Source-Vibroseis

Source : Vibroseis. AVH-IV

Electronics : VE464

Peak force : 60,000 lbs

Sweep frequency : 7-70 Hz

Sweep type : linear

Sweep Length : 20 seconds

Polarity : SEG standard

Source array-Vibroseis

Number of sources/group : 1 fleet of 4 vibrators

Array type : in-line, centered on SP flag

Number of Vibrators : 4

Recording

Recording instrument : Sercel 428

Channels recorded : 320

Record length	: 6 seconds
Sample rate	: 2ms
Data format	: SEGD 8058 revision 1

Parameters in figures

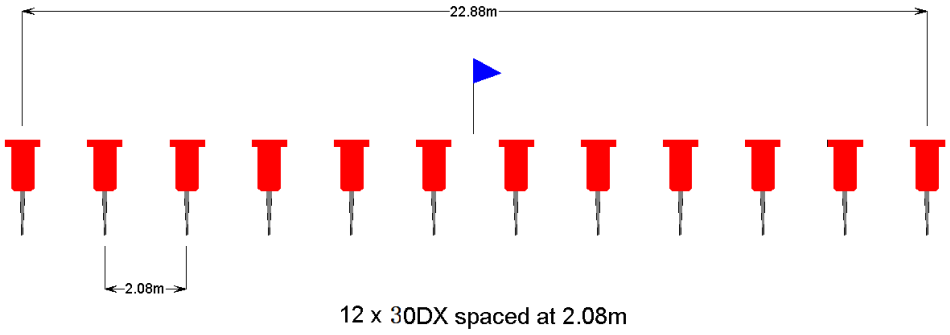

Figure 1-4: Receiver array.

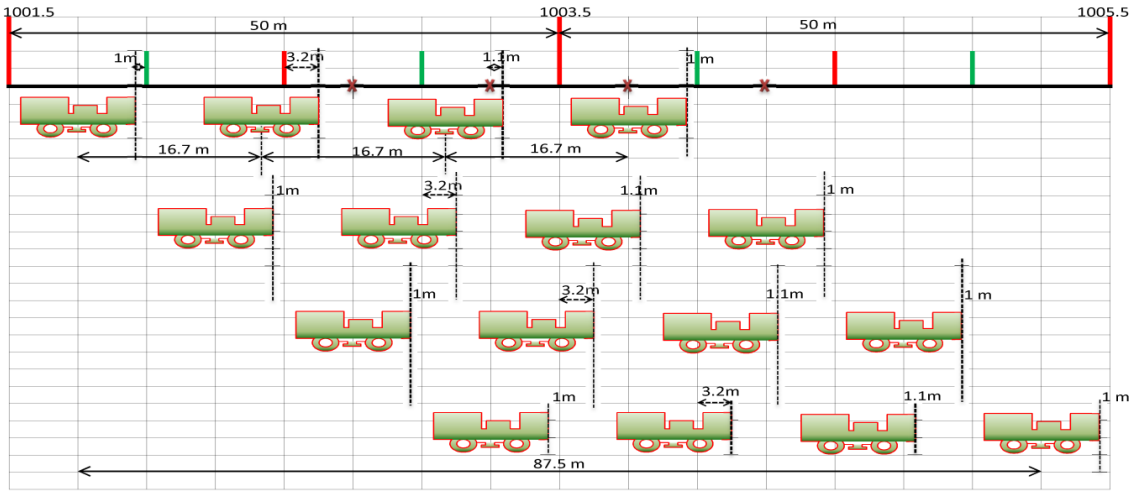

Figure 1-5: Source array.

Vista 2D/3D seismic processing version 12 software was used to carry out the data processing. The interpretation of the seismic data was done by using OpendTect version 6.0.5 free software.

The selected twelve seismic lines have a total length of 345 km. They include seismic Lines SO-03, SO-04, SO-05, SO-06, SO-22, SO-52, SO-45, SO-10, SO-11, SO-12 and SO-

13, SO-20. The lines were chosen based on the results of previous gravity analysis and the drilled wells in the basin. From the selected lines nine of them are E-W oriented and three lines have N-S orientations (Figure 1-6).

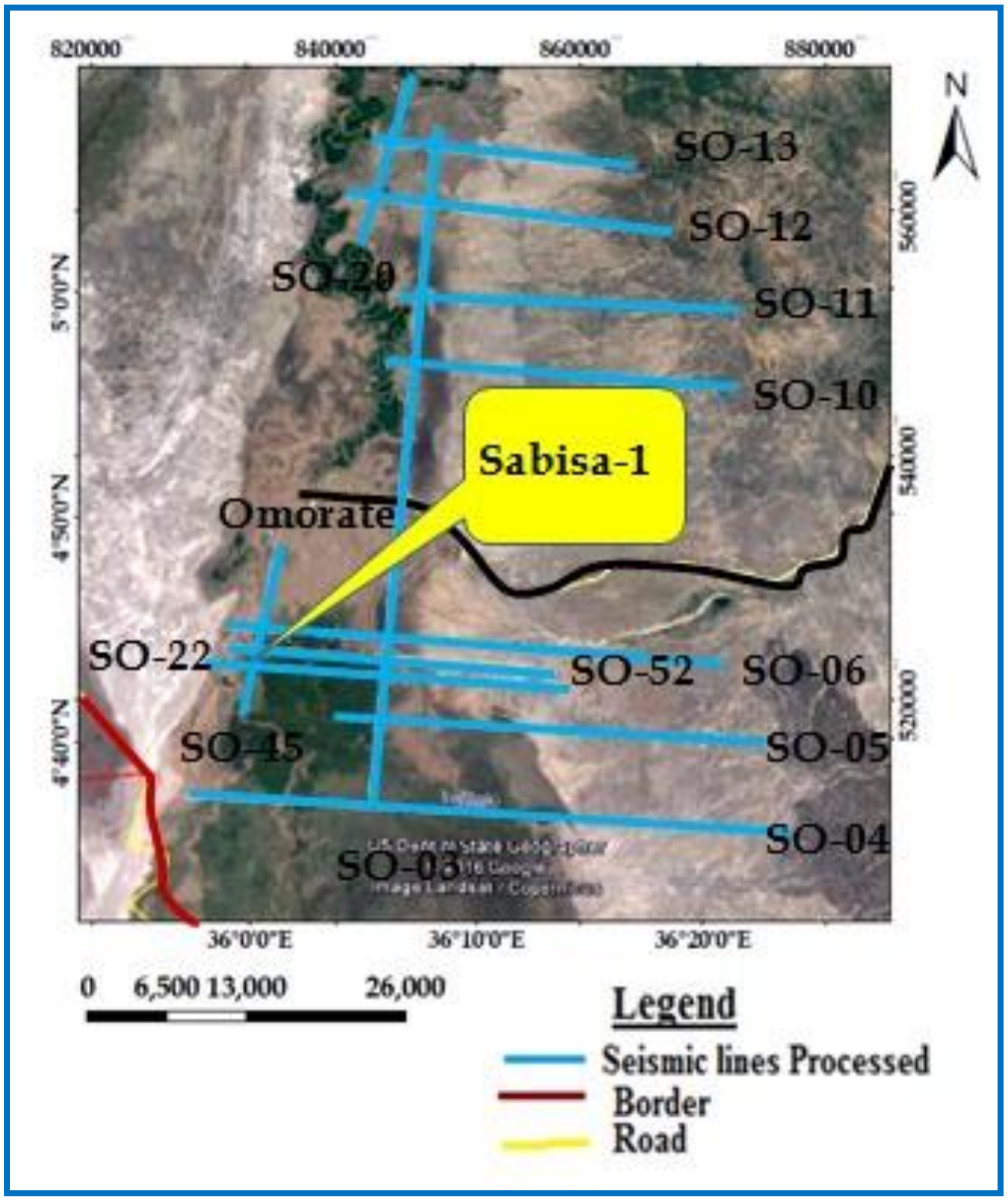

Figure1-6: Location of the seismic lines processed for this study.

1.6. Thesis Structure

The thesis comprises of seven chapters. The first chapter deals with statement of problem, location, objectives, justification and methodology of the research and

pervious works. Chapter two describes the geology of the study area. Chapter three states the theoretical back ground for seismic reflection. Seismic data processing and interpretation are discussed in chapter four and five respectively. The discussion of interpretation is described in chapter six. Finally, conclusions and recommendations are given in chapter seven.

1.7. Previous Geological and Geophysical works

According to Kazmin (1973; refered from Butzer, 1971) stratigraphic formations of Lower Omo area were described in detail to be of Pliocene-Quaternary sediments. Mapping of geological units of Omo basins are discussed in detail on preliminary report of Omo River report (Davidson et al., 1973). The summary for the extensive work done by the Canadian Geological survey Team with Ethiopian Geological Institute personnel in 1972 up to 1974 to study Petrography, Geochemistry and Geochronology under the project named "The Omo River project" was compiled by Davidson (Davison, 1983).

Ebinger and Ibrahim (1994) suggested on their study that the pre-Oligocene strata were deposited during Cretaceous rifting episodes and the Anza rift continues north-west beneath Omo rift.

According to explanation of the geological map of Ethiopia by Mengesha Tefera et al. (1996), the Omo group sediments consists Mursi, Nakalabong, Unso and Shungura Formations. They are Pliocene -Pleistocene continental deposits.

Crustal model of gravity for Omo basin by Abera Tessema (1996) reveals the presence of 2.8 km sediments and shows westward tilting of the Omo rift. In addition, contrast made between Main Ethiopia Rift (MER) and Omo rift system indicates that the Omo rift is characterized by subsided shoulders and is seismically less active while the MER system is characterized by uplifted flanks and the rift floor is seismically active.

According to Ermyas Nigusse et al., (2002) the basement is exposed about 300m away from Turmi town. Sediments are observed at about 30 km on the profile of Turmi on the road to Omorate.

The gravity data analysis carried out by Tilahun Mammo (2012) reveals that the Omo basin is an asymmetric graben-like structure built within the generally N-S trending normal faults.

The basin is the northern extension of the Turkana rift and is well studied owing to the occurrence of abundant vertebrate fossils including hominids (Brown, 1969, Tesfaye Kidane et al.,2014 and Abbate et al., 2015,).These studies have greatly increased the knowledge and understanding of the fossiliferous Plio-Pleistocene Shungura Formation.

CHAPTER TWO

2. GEOLOGICAL SETTING

2.1. Geology of South Omo Basin

Geology of the South Omo basin including the study area is shown in Figure 2-1. The study area consists of the following rock units: Layered gneiss and amphibolite, Fejej Formation, Omo Group, Kibish Formation, Nakwa Formation, Alluvial, fluvial and lacustrine Quaternary sediments.

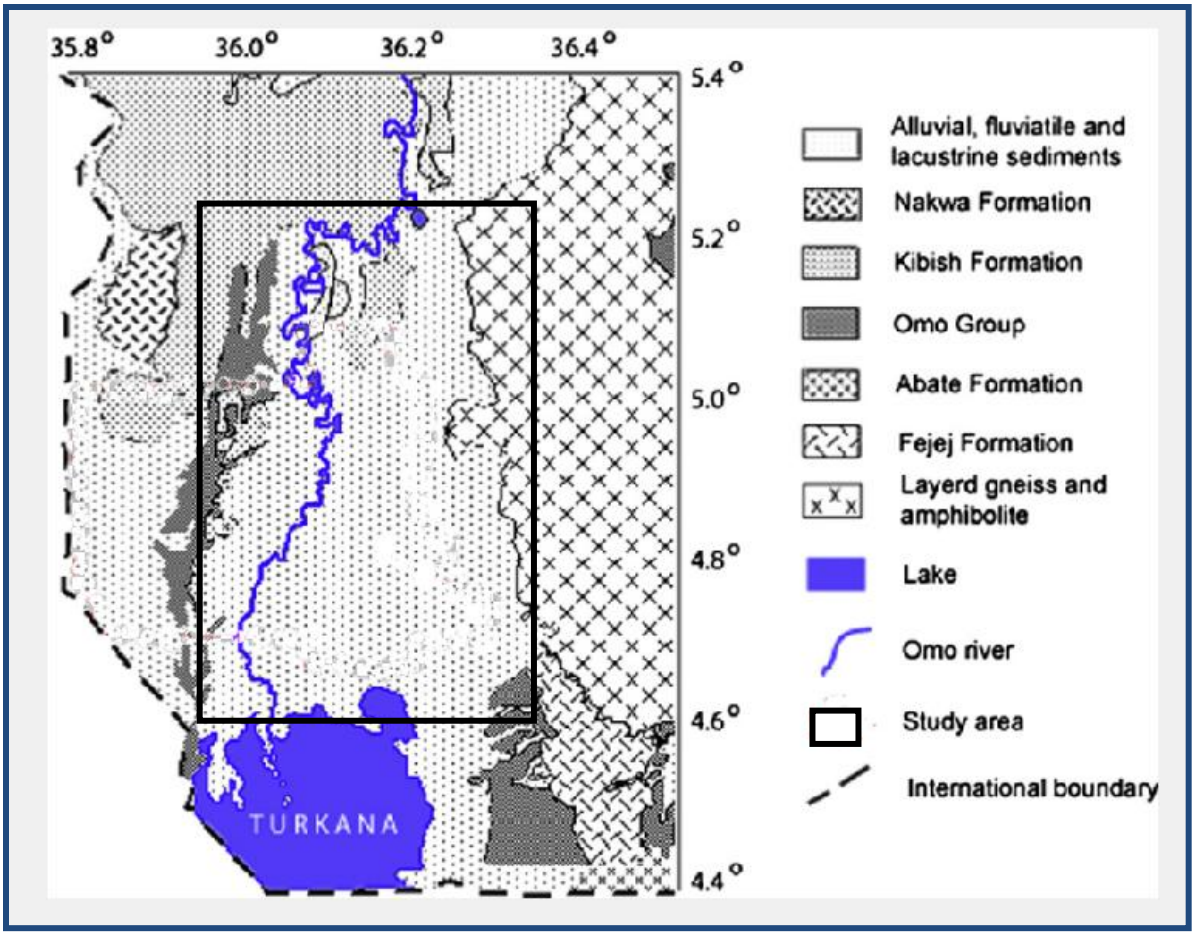

Figure 2-1: Geological map of South Omo basin (after Davidson, 1973 and Tilahun Mammo, 2012).

2.1.1. Crystalline Basement rocks

The Basement rocks **(***layered gneiss and amphibolite***)** consist of gneisses exhibiting polyphase deformation and high-grade metamorphism (Davidson et. al, 1973). They are intruded locally by syn and post-tectonic plume mainly granitic in composition, although minor gabbroic and ultra-mafic intrusions are present. Metamorphic grade is mainly middle to upper amphibolite faces.

According to Davidson et al 1973, the following four units occur in granulate faces on the eastern part of the Omo River.

a) Mafic granulite or relatively mafic horn blended gneisses and amphibolite referred as a Konso gneisses by Kazmin 1973.
b) Well layered biotitic gneisses containing clearly recognizable meta-sedimentary components.
c) Dominantly grey biotitic –horn-blended genesis of variable color index, well defined masses of relatively uniform orthogenesis of granodioritic, tonalitic and dioritic composition.
d) Pale pink to light grey quratzo-feldspathic gneisses, generally leucocratic and having granitic composition.

2.1.2. Fejej Formation

Fejej Formation lies on the crystalline basement to the east of Omo River near Lake Turkana. It is not more than 150m thick. Fejej Formation flows are in part columnar and some are less than 20m thick. The flows dip very gently southwest ward along their northern margin. But to the south are wrapped about north trending axes. In the main exposure area the Fejej and succeeding formations are cut by several sets of faults with minor displacements. Some Fejej basalt flow nobly weathering surfaces with dark parasol and at one place, thin lighted tuffaceous sediment. The basalt flows are very similar to one another, the basalt is dark grey, aphanite's to very fine grained, generally aphyric through locally carrying plagioclase phenocrysts (Davidson, 1983).

2.1.3. The Omo Group

The Omo Groups are categorized under the deposits of Pleio-Pleistocene (Davidson, 1983). The Stratigraphy of the Omo Groups is exposed at the southern end of Nkalabong range. The Omo group consists of four Formations. These are: Mursi Formation, Nkalabong Formation, Usno Formation and Shungura Formation.

2.1.3.1.The Mursi Formation

According to Davidson et al., (1973) by providing the reference (Butzer, 1971, p, 9), the Mursi Formation rests unconformably on west-dipping rhyolites. It is categorized in to two units: the lower unit is sedimentary and the upper unit is flood basalt. The lower sedimentary unit has three members. These are

- West tilted pre-rift rhyolites of probable Miocene age.
- 150m of clay ,silts and sands and
- With subordinate tuff and pebble beds.

These sediments conformably overlain by flood basalts dated at 4.2 mA. This Mursi basalt composed of relatively few, thin, columnar flows of dark grey basalt, locally scattered plagioclase phenocrysts and chlorite filled amygdule. Lacustrine sediments at lower Miocene age which are inter-bedded with tuffs lie above the Fejej basalts along the eastern part of Lake Turkana (Assefa Akililu & Kibebew Fantu, 1999). It is deltaic and fluvial-littoral lacustrine beds with thickness of 143m (Kazmin, 1973).

2.1.3.2.The Nkalabong Formation

It is located at the southwest end of Nkalabong range, where a section approximately 90m thick is exposed (Davidson, 1983). Grey to brown fluvial clastic sediments lie on weathered and faulted Mursi basalt. In the lower part of Nkalabong formation is built by fluvial sediments which pass up in to colian and then lacustrine literal rocks (Kazmin, 1973). Both Mursi and Nkalabong formation are overlain with mild unconformity by Kibish formation.

2.1.3.3.The Usno Formation

It is small areas of sediments that are exposed along the west bank of the Omo River beneath the quaternary Kibish Formation. Usno Formation comprises of 200m of alternating fluvial and

lacustrine sediments with thin tuff horizon. It is tilted a few degrees to the west and overlain with shallow angular unconformity by the Kibish Formation.

2.1.3.4.The Shungura Formation

It is Pleistocene sediments (Kazmin, 1973). Shungura Formation is exposed for about 60 km along west side of the Omo River north of Lake Turkana. Shungura Formation includes 760 m of brown, grey and buffy clays, silts, sands, gavels, tuffs marts and fresh water lime stones. Like Usno, Shungura Formation sediments, it is filled gently to the west and is overlain with shallow unconformity by Kibish Formation. The sedimentation recorded is one of fluctuating fluvial and lacustrine cycles.

2.1.4.The Kibish Formation

It is deposited during Pleistocene-Holocene age. Kibish Formation is named by Butzer (1971) cited by Davidson (1983). It is well exposed where the Omo River and its ephemeral side tributaries have cut through. Kibish Formation has four members of 120m thickness.

Member I

It is the lower unit 31 m thick that has gravelly sand at the base followed by alternating clay, silt and sand.

Member II

It is 22m thick. The sediments composed predominantly massive silts, deposited on basalt tuff that blanketed the dissected surface of member I.

Member III

It is 46 m thick. The sediments are clays, silts and sands with thin shale beds associated with the second cycle.

M**ember IV**

It is divided in two units. The First unit is 13.5m sands, silts and clays with gravel base. The second unit is 8m of sands, silts with minor tuffs.

2.1.5.The Nkawa Formation

It is cones standing 400m thick of volcanic rocks of basic alkaline affinity named Nkawa Formation. The main lava is basanite with minor tephrite, both carry phenocrysts of plagioclase and augite. It lies 55 km northwest of Lake Turkana.

2.1.6.Quaternary sediments

It is Holocene age sediments. Quaternary sediments are widely spread all over the country and belong to various genetic types. The South Omo area is alluvial, fluvial and lacustrine sediments (Kazmin, 1973).

CHAPTER THREE

3. SEISMIC REFLECTION METHOD

3.1. Theory of Seismic Reflection

Seismic data is generated by sending artificial energy into the Earth and recording its return. In the early days, waves are produced by blasting in shallow wells but today vibrations with different range of frequencies for wave generation are used.

A seismic wave is an elastic wave that travels through the solid rock. There are two types of seismic body waves that travel in solid rocks.

a) Longitudinal (Primary or compression) P- waves are waves that propagate by moving the particles in the medium parallel to the direction of propagation.
b) Transverse (secondary or shear) S-waves are propagate by moving the medium particles perpendicular to the direction of propagation.

Among the seismic body waves, only **the longitudinal waves** can travel in fluids. A seismic wave propagating in the earth encounters several discontinuities between rock types that have different physical properties. It produces wave phenomena such as reflections, diffractions, absorptions, scattering and transmissions (refractions).

At the interface between different rocks, a part of the incident energy is reflected back to the surface and rest of energy is transmitted the underlying rocks.

The relative sizes of the transmitted and reflected amplitudes depend on the contrast in acoustic impedances of the rocks on each side of the interface. The acoustic impedance (Z) of the rock is the product of its density (ρ) by (V) P-wave velocity (Gadallah and Fisher, 2009).

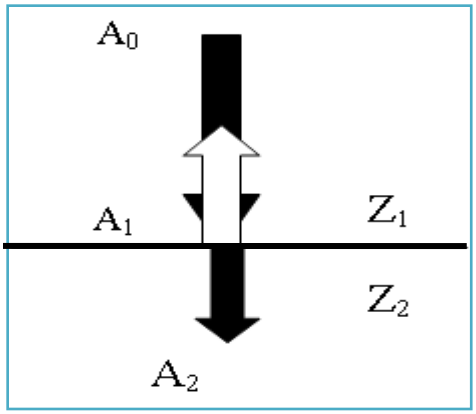

Figure 3-1 Normal - incidence reflection coefficient (Gadallah and Fisher 2009).

Consider P-wave amplitude A_0 that is normally incident on an interface between two layers having seismic impedances of Z_1 and Z_2 (Figure 3-1). The transmitted ray has amplitude A_2 that travels the interface in the same direction as incident ray. The reflected ray has amplitude A_1 that returns to the source along the path of the incident ray. The Reflection coefficient R is the ratio of amplitude A_1 of the reflected ray to the amplitude A_0 of the incident ray,

$$R = \frac{A_1}{A_0} = \frac{Z_2 - Z_1}{Z_2 + Z_1} \tag{3.1}$$

The Transmission coefficient is the ratio of the amplitude transmitted to the incident amplitude.

$$T = \frac{A_2}{A_0} = \frac{2Z_1}{Z_2 + Z_1} \tag{3.2}$$

The seismic method adapts the theory of optics to study the propagation of the seismic energy in the earth. Snell's law of reflection is fundamental to understanding the seismic energy propagation. Huygens's principle provides view of seismic energy propagation and attenuation. Fermat's principle introduces the possibility of multiple travel paths between source and receiver that may give rise to more than one primary reflection event.

Theory of seismic method is discussed in detail by many text books (Kearey et al., 2002; Nanda, 2016 and Telford et al., 1990). Seismic methods for exploration of hydrocarbons use mostly primary wave reflecting from the subsurface.

3.2. Seismic Reflection Data Processing

The main purpose of data processing is to get interpretable result of the 2D seismic data. Seismic data is interpreted to provide information about composition, fluid content, extent and geometry of rocks in the subsurface. Seismic data can be used in many ways such as regional mapping, prospect mapping, reservoir delineation, seismic modeling. Additionally, it helps for direct hydrocarbon detection and the monitoring of productive reservoirs. However, this cannot be done without mentioning basic mathematical concepts in processing techniques that are commonly applied to 2D seismic data before interpretation.

Mathematical theory and concepts

Much of the seismic data processing is based on the branch of Mathematics called statistical communication theory. Since seismic data are recorded as sampled data, integration reduces to summation and differentiation to subtraction.

Time (T), Frequency (F), Space (X) and wave number (K) Domains

In seismic data processing the signal can be described equally well in a time series (amplitude versus time) or as combination of an amplitude spectrum (amplitude versus frequency) and phase spectrum (Figure 3-2).

To convert from time domain to frequency domain requires to use the Fourier Transform and to change from frequency domain to time domain requires the use of Inverse Fourier Transform. For recently collected sampled or digital data simple and fast methods of transformation are utilized. These are known as Fast or Finite Fourier Transform (FFT) and Inverse Fast or Finite Fourier Transform (IFFT).

$$G(w) = \int_{-\infty}^{+\infty} g(t) e^{-jwt} dt \qquad \text{Fourier Transform of g (t)} \qquad (3.3)$$

$$g(t) = \frac{1}{2\pi}\int_{-\infty}^{+\infty} G(w)e^{jwt}dw \qquad \text{Inverse Fourier Transform of G (w)} \qquad (3.4)$$

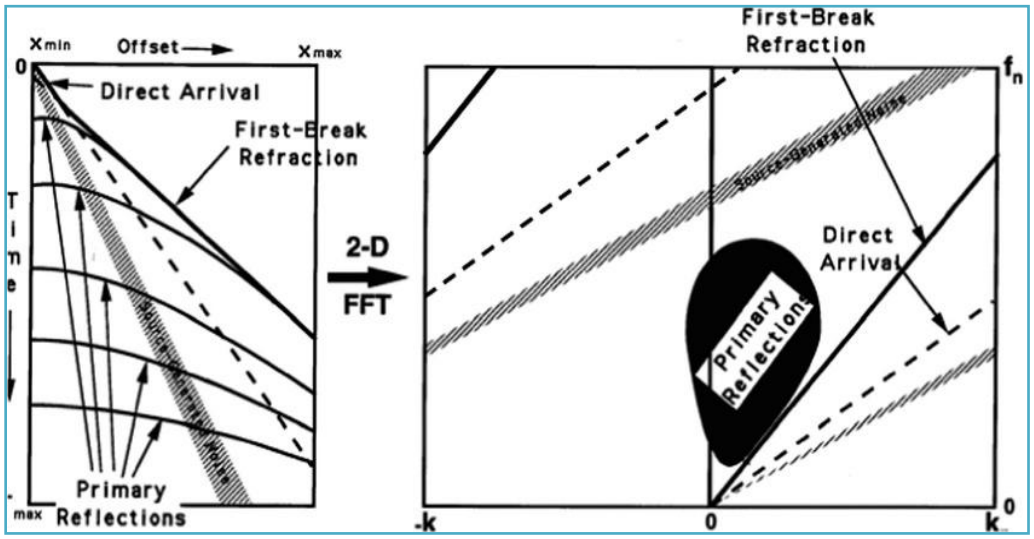

Figure 3-2: T-X and F-K domain representations of the various seismic arrivals (after Gadallah and Fisher, 2009).

Therefore, in seismic data processing applying FFT is the useful tool for transformation from Time and space domains (T-X) to the frequency and wave number (F-K) domains (Figure 3-3).

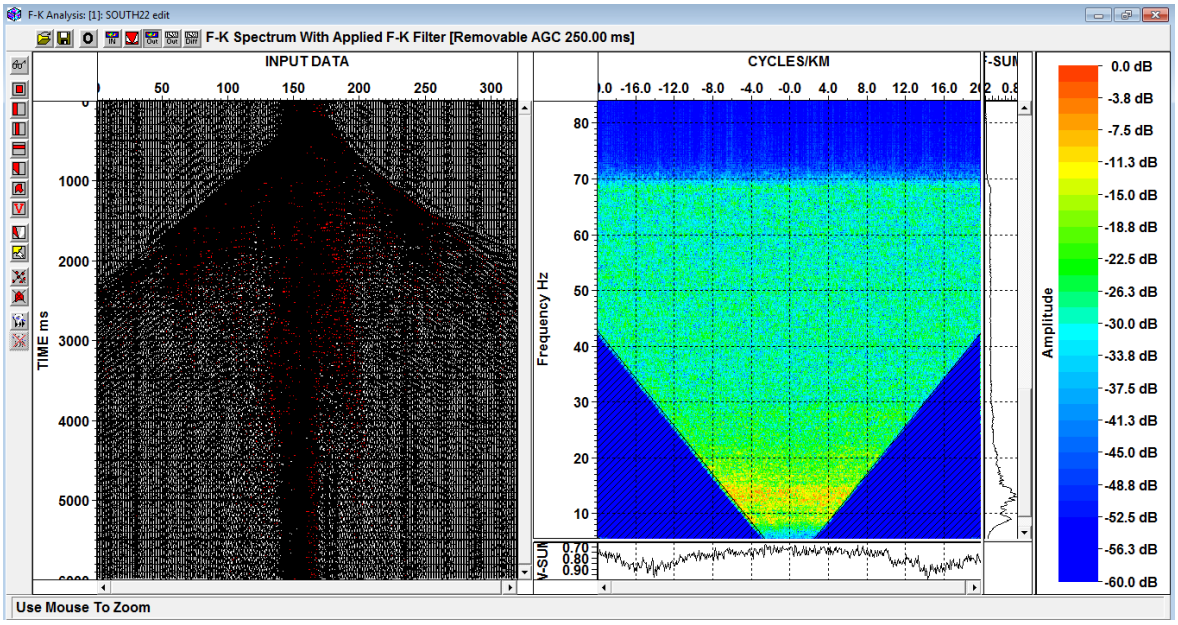

Figure 3-3 T-X and F-K domain representation of processed South Omo data.

Note that the signals are crossed by noise in the T-X Plane whereas they are separated in the F-K plane (Figure 3-2).

Filtering, Convolution, Deconvolution and Correlation

The surface of the earth is in constant motion because of both natural phenomena and cultural activities. This results the background of the earth motion is also recorded along with the desired motion produced by the seismic sources. This undesired recording is called Noise. The ratio of Signal amplitude to Noise amplitude is known as the Signal to Noise Ratio (S/N). In the recorded data it is vital to have S/N is greater than or equal to 1, but in most cases S/N ratio is less than one at lowest frequencies and at highest frequencies. One method of obtaining the desired result is to apply a **filter** that greatly attenuate frequency components where S/N is less than one. Such filter is called band-pass filter.

Convolution is the mathematical operation that defines the shape of wave form as a result of its passage through a filter. The effect of the filter can be categorized by its impulse response. The impulse response is a wave form in the time domain, which can be transformed in frequency domain by Fourier transform. The mathematical operation for convolution is given by equation (3.5) as follows. If the input signal g(t) is convolved with impulse response f(t), with convolution operator (*) to filter, then the filtered output y(t) is obtained.

$$y(t) = g(t) * f(t) \tag{3.5}$$

Deconvolution is the process that counteracts a previous convolution action. Deconvolution is an important task in seismic data processing, will be discussed in the next Chapter in detail.

Cross-correlation of two digital waveforms involves cross–multiplication of the individual waveform elements and summation of the cross-multiplication products over the common time interval of the waveforms.

Autocorrelation is when the wave form cross-correlated with itself, to give the autocorrelation function.

3.3. 2D Seismic Data Interpretation

The next step of seismic data processing is to interpret the result obtained from data processing. Seismic interpretation is the analysis of seismic data to generate reasonable models and predictions about the structures and properties of subsurface. Techniques used in seismic interpretation are discussed in detail (Gadallah and Fisher, 2009). During the structural interpretation of seismic data, interpreters preview the data in order to identify subsurface structures, such as rock layers and faults. Rock layers are the result of long time sedimentation processes, and consequently, each layer forms a surface that approximately corresponds to the earth's surface at certain time in the past. A discontinuity in the layered surfaces reveals faults or channels.

Interpretive processes are now accomplished by using modern interpretation software packages, such as the kingdom suite software of Seismic Micro Technology (SMT) or OpendeTect software of dGB Earth Sciences.

3.3.1. Horizon interpretation

Horizon interpretation deals with identifying sequence boundaries (horizons) which are observable on seismic line. Horizons are tracked with regular patterns of seed lines to approximate the small portion of data continuity. Auto trackers widely assist in most horizon interpretation however; manual picking method was used for horizon interpretation.

3.3.2. Fault interpretation

Fault interpretation is about defining fault surfaces, along which rock layers are displaced relative to each other. Fault surfaces are identified by finding termination in continuous horizons. The fault interpretation procedure is a time consuming task.

CHAPTER FOUR

4. SEISMIC DATA PROCESSING

Seismic data processing requires an orderly approach to converting raw field records into meaningful information about the subsurface geology. Before beginning data processing for a given prospect extensive testing on the data should be done. This involves design of the optimum parameters at each step in the processing. The major steps of processing seismic data are shown in Figure 4-1.

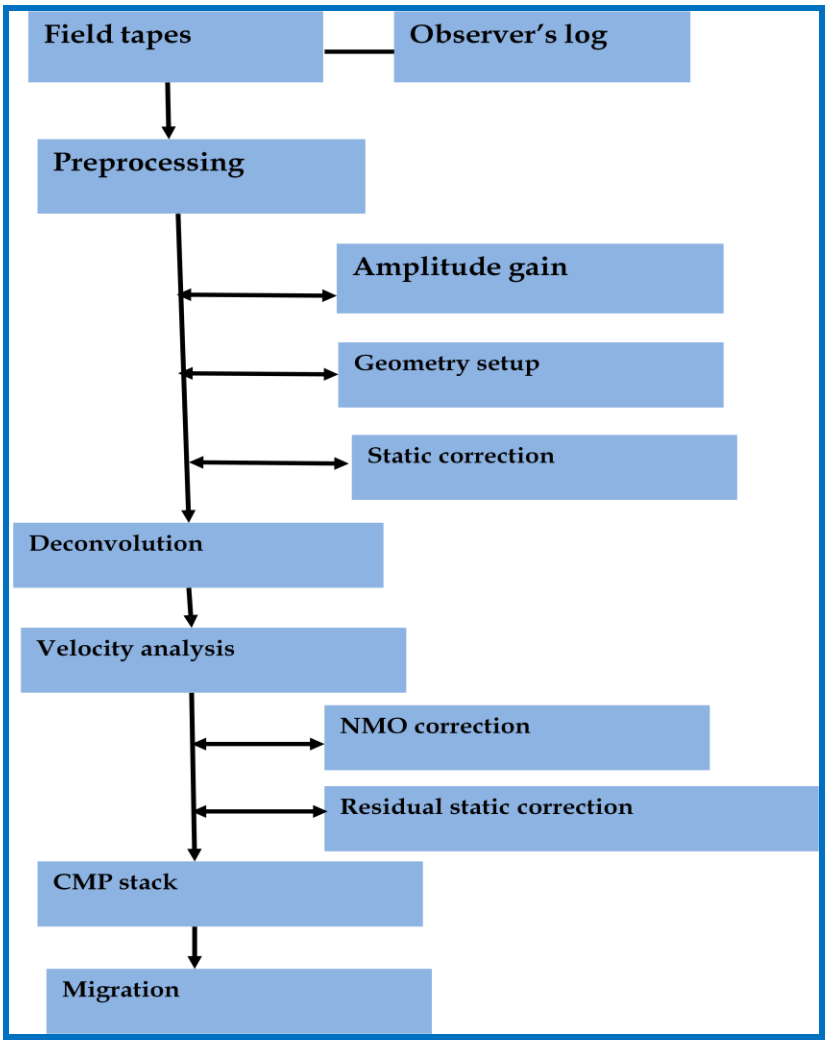

Figure 4-1: Flow chart of seismic data processing.

4.1. Preprocessing

In preprocessing the format of the acquired data is converted from field format (SEGD) to the (SEGY) format. All shot records are then displayed to make sure documentation provided by the field crew is accurate. This will help to identify the problems in the raw data.

4.2. Amplitude Gain Control (AGC)

The amplitude of the reflections decreases gradually with depth due to spherical spreading and absorption. Therefore, it is crucial to correct the amplitude. The correction of amplitude is known as gain function. Automatic gain control (AGC) is applied to correct the amplitude. The parameter of used AGC is 250ms. During AGC noises (ground roll and other noises) are magnified. Figure 4-2 shows the effect of AGC on Shot point 1557.7 of line SO-22.

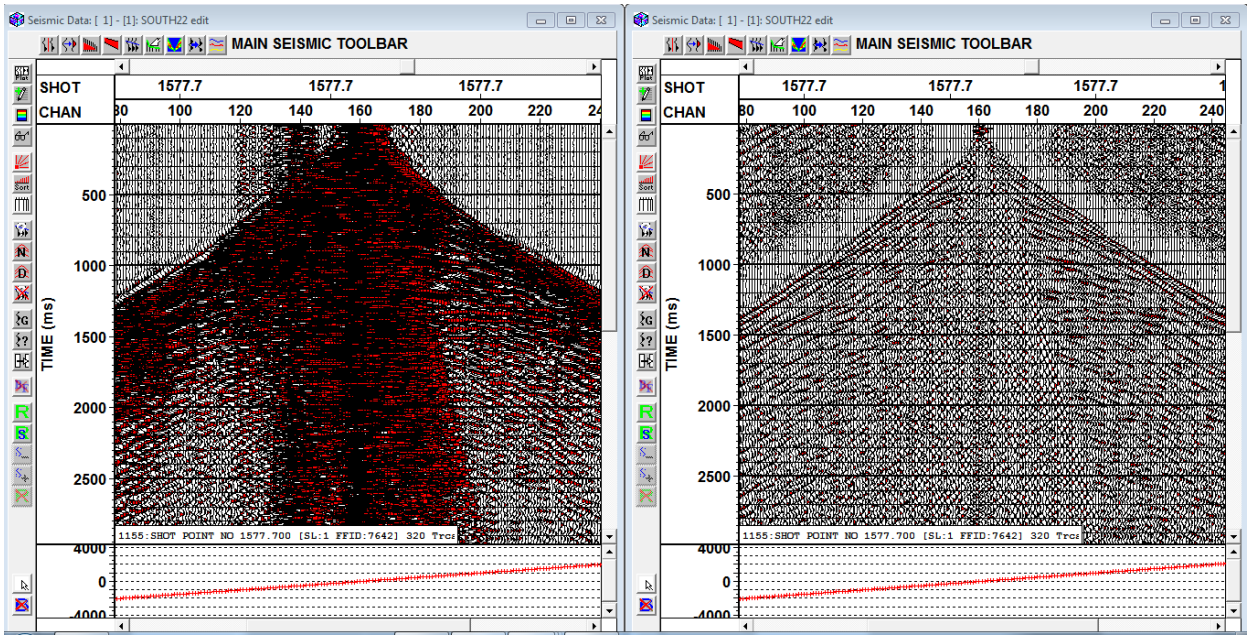

Figure 4-2: Field records of shot point 1557.7 on Seismic Line SO-22 before and after applying AGC.

4.3. Geometry setup

The next step is to create a geometry database. The starting point of the database is to

a) Accept an X-Y coordinate system
b) Allocate unique numbers to and specify coordinates for all source and receiver positions.

For parameter testing and selecting the field the shot format has to be sorted in to common midpoint (CMP) format. Figure 4-3 illustrates an example of the working environment for data sorting.

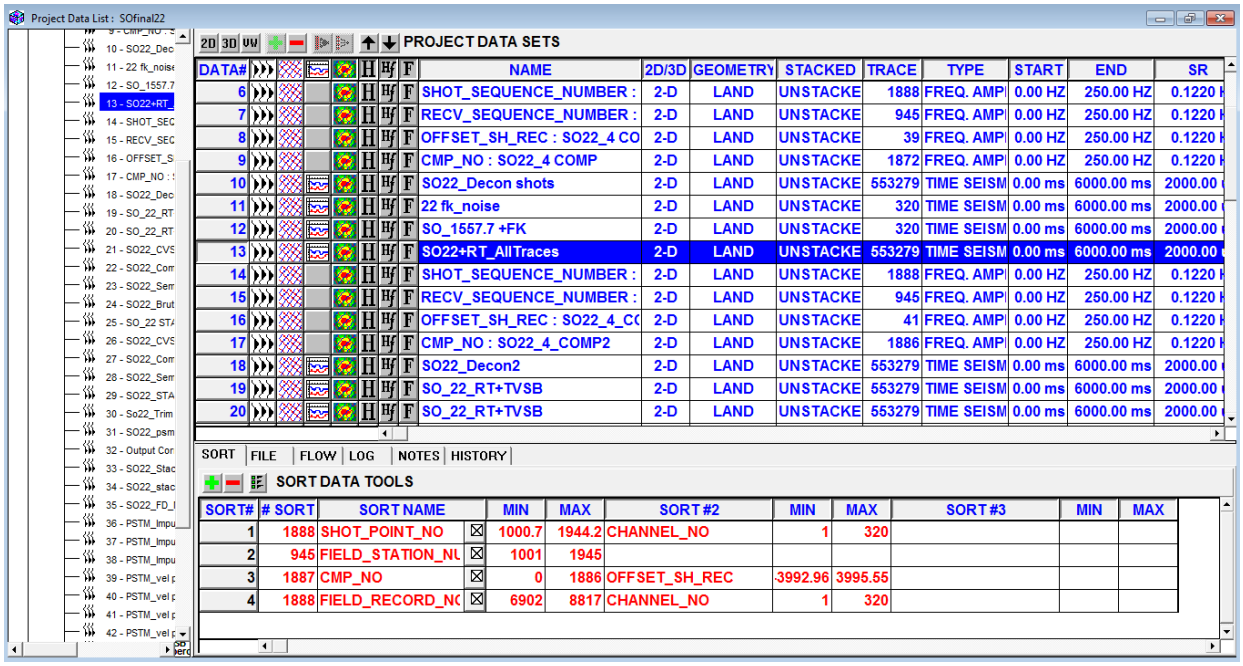

Figure 4-3 Illustrate working environment for data sorting for line SO-22.

4.4. Static Corrections

Static corrections are made to seismic reflection data to compensate for time shifts in the data caused by changes in topography and variations in near-surface seismic-wave velocity (weathering zone) or reference to datum (Schuster, 2010). Figure 4-4 shows the static corrections for 500 CMP on the Line SO-22. The improvement in coherence of the arrivals can be observed.

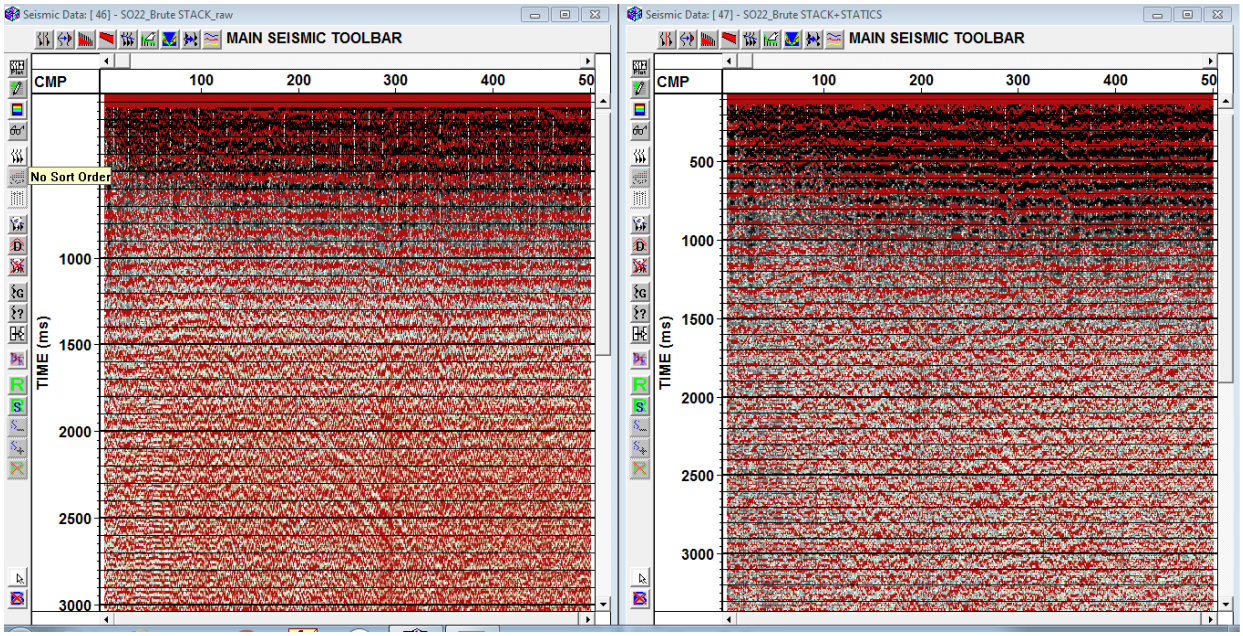

Figure 4-4: Seismic Line SO-22 before and after static correction.

4.5. Deconvolution

Deconvolution is the processes that improve the vertical resolution of seismic data by compressing the basic wavelet, which also increases bandwidth of the wavelet (Gadallah and Fisher, 2009). Additionally, deconvolution can be used to attenuate ghosts, instrument effects, reverberations and multiple reflections. Many components of seismic noise lie within the frequency spectrum of the reflected pulse and therefore cannot be removed by frequency filtering. Inverse filtering (deconvolution) discriminates against noise and improve signal character. Deconvolution is the analytical process of removing the effect of some previous filtering operation (convolution). Inverse filters are designed to deconvolve seismic traces by removing the adverse filtering effects associated with the propagation of seismic pulses through the layered ground or through the recording system.

Surface consistent deconvolution

It uses redundancy of multifold data to statistically determine and attenuate effects on signal wave form that occur in the vicinity of the each source and receiver position (Gadallah and Fisher, 2009). Figure 4-5 indicates the effects on 500 CMP of seismic Line SO-22 before and after surface consistent deconvolution applied.

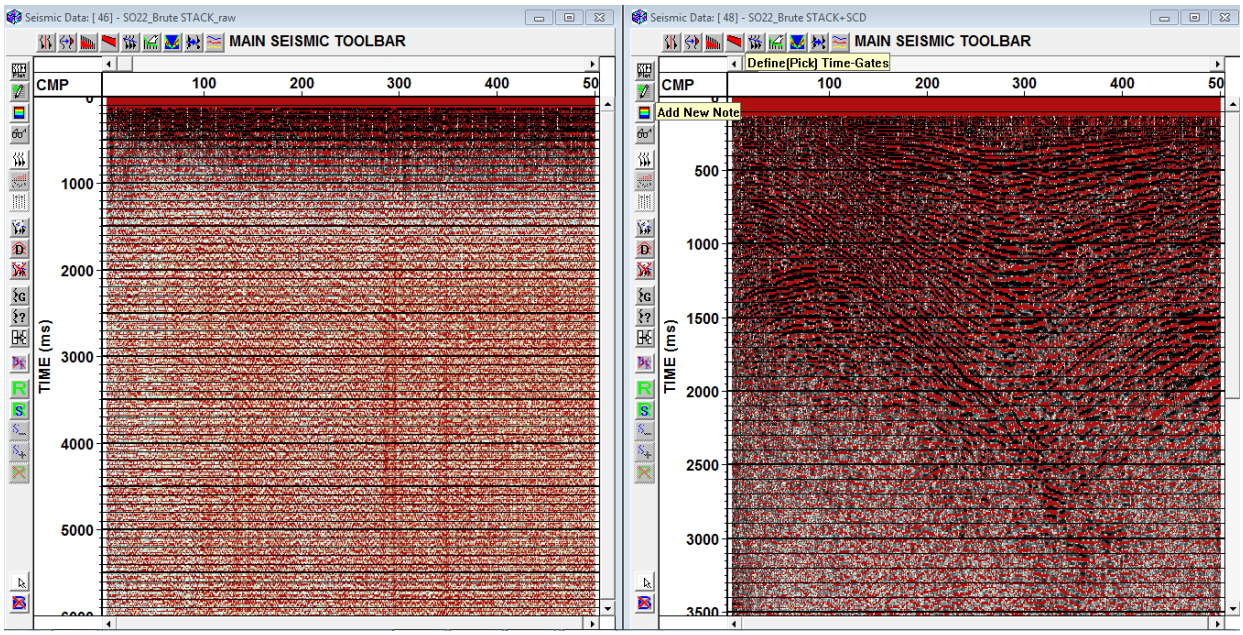

Figure 4-5: Seismic data before and after surface consistent deconvolution.

Time Variant Spectral Balancing (TVSB)

It corrects for inelastic attenuation by dividing the input into relatively narrow frequency bandwidths and applying AGC to each (Gadallah and Fisher, 2009). The separate frequency bands are then recombined in such a way as to preserve original amplitude levels. Figure 4-6 illustrates the difference between the seismic Line SO-22 of shot point 1557.7 before and after the TVSB applied.

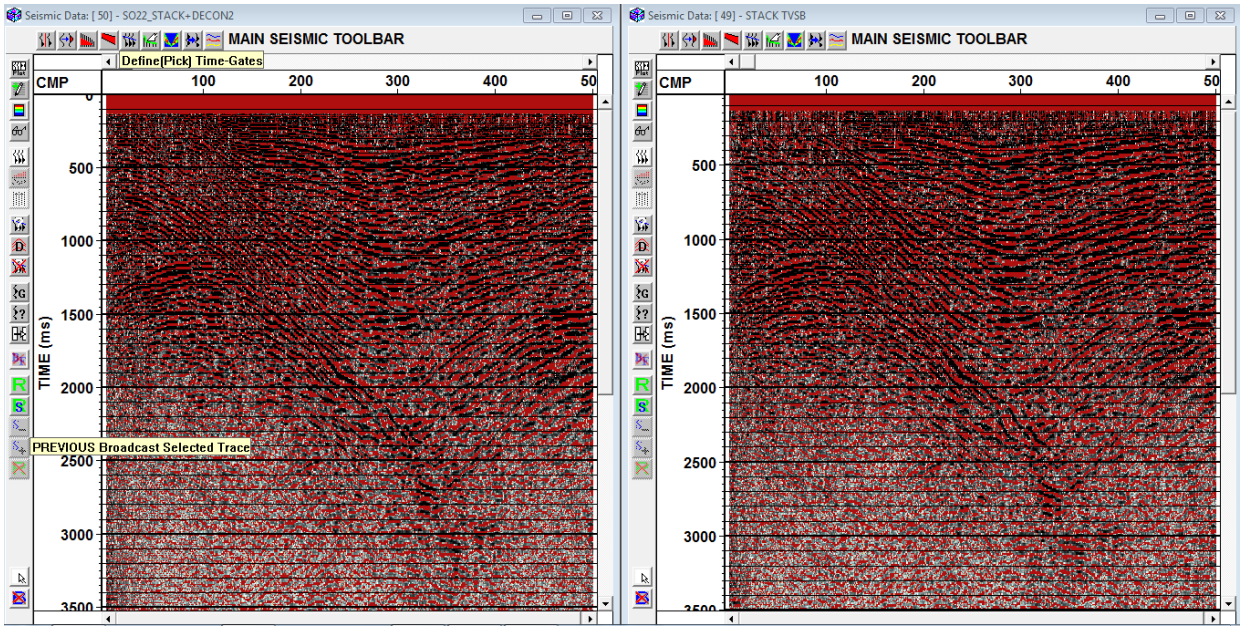

Figure 4-6: Seismic Line SO-22 before and after TVSB.

4.6. Velocity analysis

In seismic literature there are different types of velocity. These are instantaneous velocity, interval velocity, average velocity, RMS velocity, NMO velocity, Stacking velocity, migration velocity and apparent velocity (Gadallah and Fisher, 2009). The most important velocities in seismic processing are apparent velocity, average velocity, NMO velocity and migration velocity. Several types of velocity analysis have been used over the years. The more commonly used and utilized methods in this thesis are

a. T^2-X^2 analysis
b. Constant Velocity stack (CVS)
c. Velocity spectrum method

T^2-X^2 analysis: In this method, time (T) of the selected primary reflections on each trace squared and plotted against the square of the offset (X) corresponding to the traces on which times were picked.

$$T_x^{\,2} = \frac{X^2}{V^2} + T_0^{\,2} \qquad (4.1)$$

The slope of the straight line is $1/V^2$ and the intercept at X=0 is T_o^2. The plotted lines may not fall exactly along the straight line that is fitted them. The least square fitting method is used to define slope for all significant primary reflections. It is a reliable way to estimate stacking velocity.

Constant Velocity Stacks (CVS): Stacking velocities are estimated from CMP gathers by evaluating stacked event amplitude and continuity when a single velocity is used for NMO corrections at all the times on the record. A range of velocities defined by the lowest and highest stacking velocities expected. A set of velocities is established by incrementing by constant amount from the lowest to the highest velocity. Stacking velocities are picked directly from these panels by selecting the velocities that yield the best coherency and strongest amplitudes for velocity values at certain center times.

Velocity Spectrum Method: The initial result of velocity analysis is a set of velocity functions that are determined at specific CMP locations within the survey. The Velocity functions are defined by set of time, the velocity pairs that are picked for significant primary reflections. It is based on the correlation of the traces in a CMP gather. The velocity spectrum distinguishes the signal along the hyperbola paths even with high random noise level. This method is suitable for data with multiple reflection problems, and less suitable for highly complex structure problems. Figure 4-7 demonstrate how velocity of CMP 360 on seismic Line SO-22 is picked.

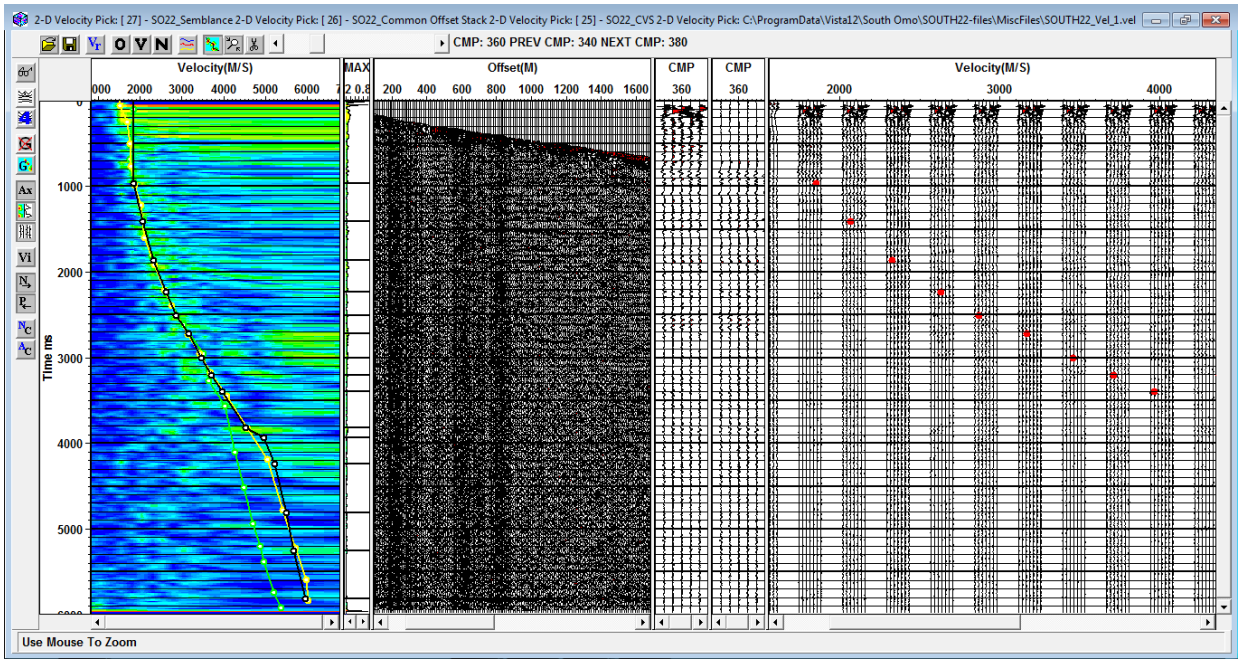

Figure 4-7: Velocity analysis for Seismic Line SO-22.

4.7. NMO Correction

The travel times associated with geophones at large offsets are greater than those at short offsets by the virtue of the increased ray path distances (Reynolds, 1997). In the case of horizontal reflector at depth z below ground level, the difference in travel time at the largest offset from normal incidence is known as the normal move out (NMO).

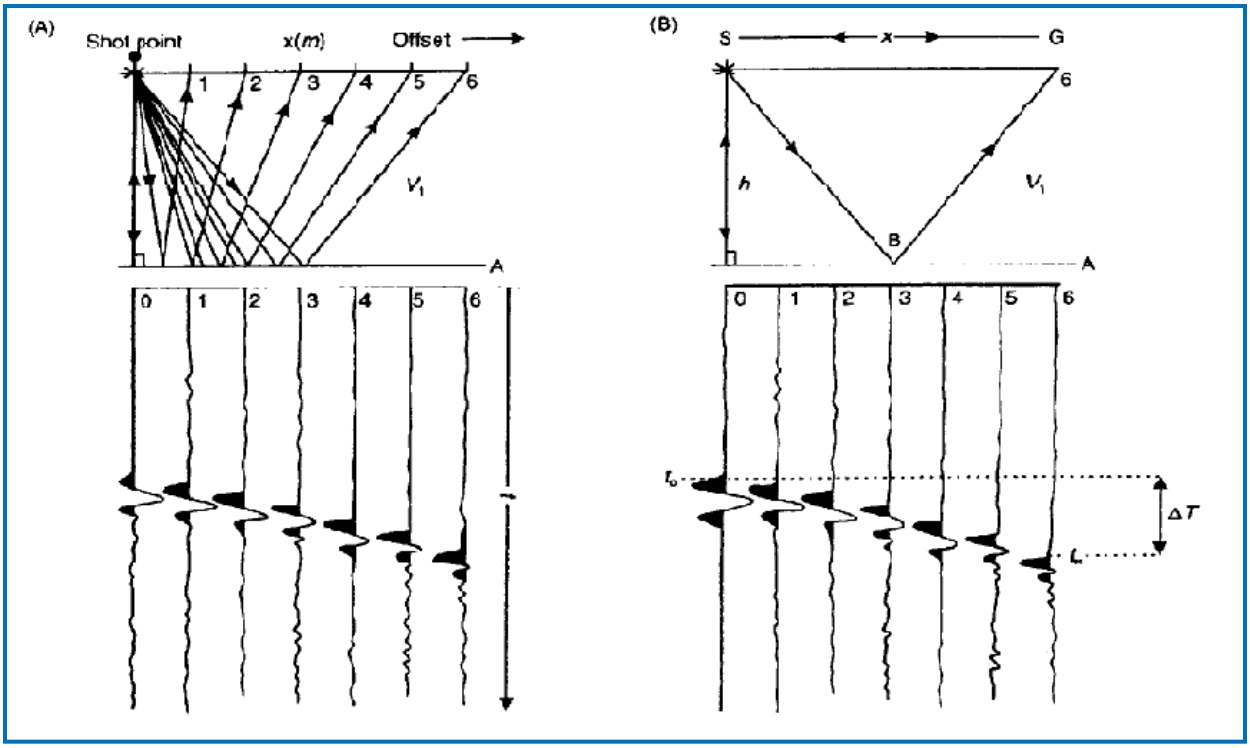

Figure 4-8: NMO Correction (after Reynolds, 1997).

4.8. Residual Static Corrections

Applying NMO and static corrections to traces within the CMP gather may not result in perfect alignment of primary reflections. Misalignment may be caused by incorrect or incomplete static corrections. To correct these misalignments an estimate of the time shifts from perfect alignment is needed.

Residual static corrections involve three stages:

1. Picking the values
2. Decomposition of its components, source and receiver static, structural and normal move out terms.
3. Application of the derived source and receiver terms to travel times on the pre-NMO corrected gathers after finding the best solution of residual static corrections.

These static are applied to the deconvolved and sorted data, and the velocity analysis is re-run. Figure 4-9 displays residual static corrections of seismic Line

SO-22. A refined velocity analysis can be obtained to produce the best coherent stack section.

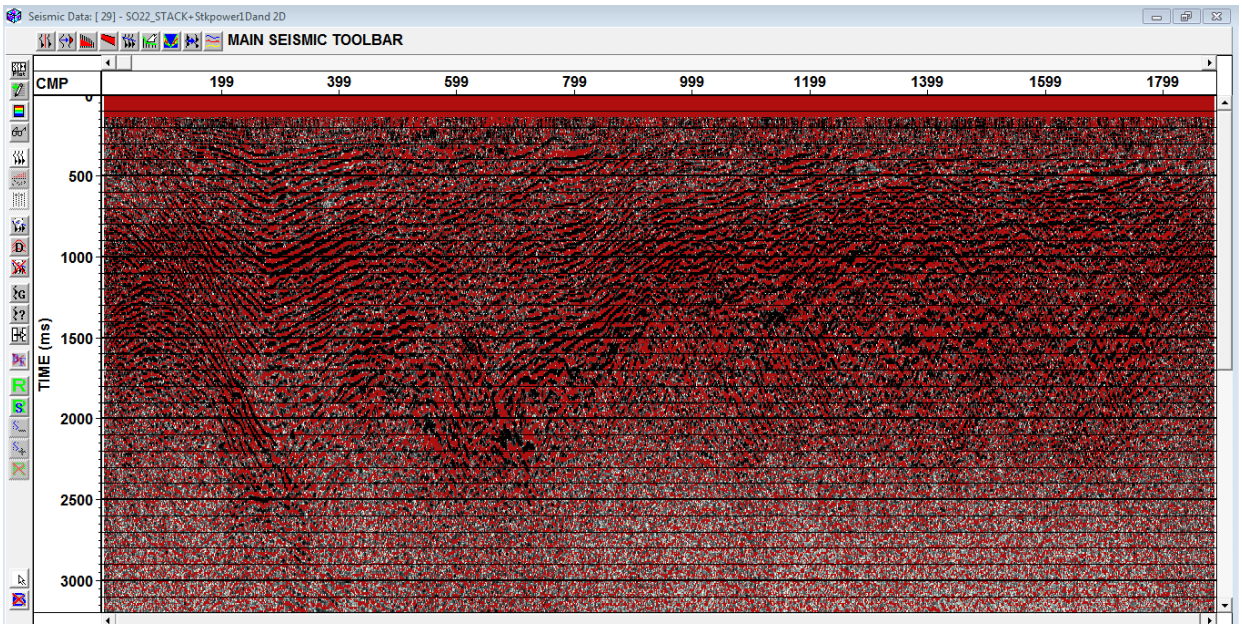

Figure 4-9: after the application of first residual static Seismic Line SO-22.

4.9. CMP Stack

Vertical stacking is performed to combine all vibrator records from single source pattern in to one record. Horizontal, CMP Stacking is the first output of seismic data processing that can be readily interpreted (Gadallah and Fisher, 2009). It combines all traces of all CDP gathers into single traces for every CMP on a line. CMP stack moves all sources and receivers to their common midpoint positions. Figure 4-10 presents CMP stack of seismic Line SO-22.

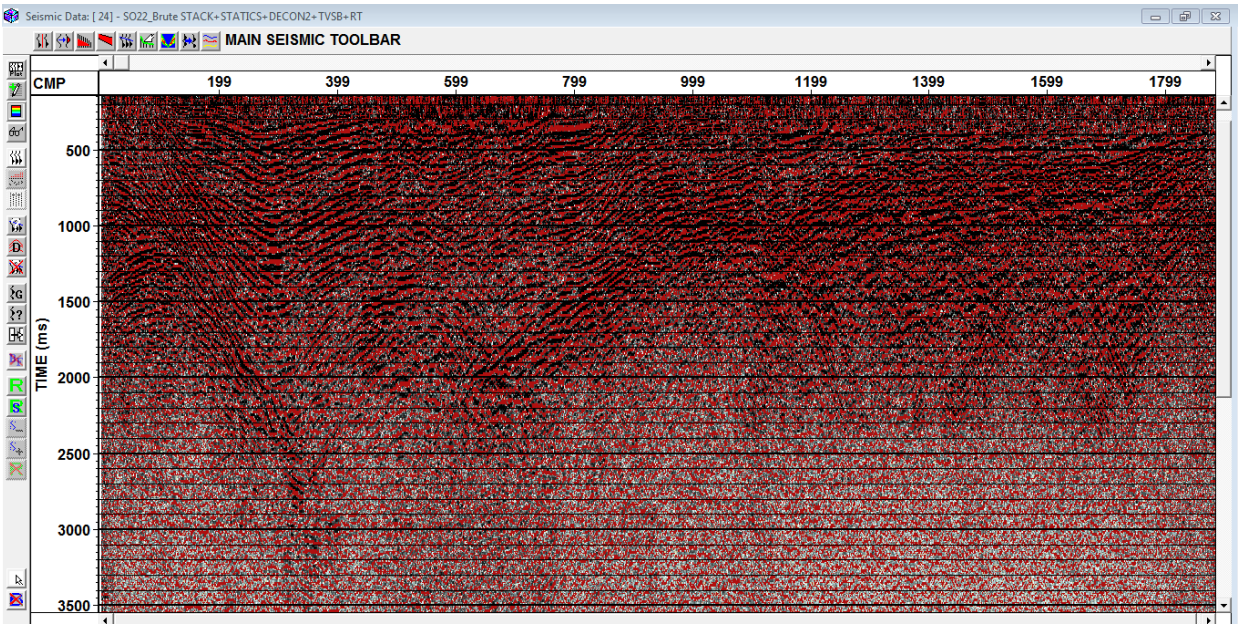

Figure 4-10: CMP stack of Seismic Line SO-22.

4.10. Migration

The objective of Seismic data processing is to produce as accurate as possible images of the subsurface targets. Migration is the process of reconstructing a seismic section so that the reflection events are repositioned under the correct surface location and at a corrected vertical reflection time (Kearey et al., 2002). Migration also improves the resolution of seismic sections by focusing energy spread over a Fresnel zone and by collapsing diffraction patterns produced by point reflections and fault beds. The basis of the migration method is Huygens' secondary source principle. The process of migration is to collapse the apparent secondary wave fronts to their points of origin.

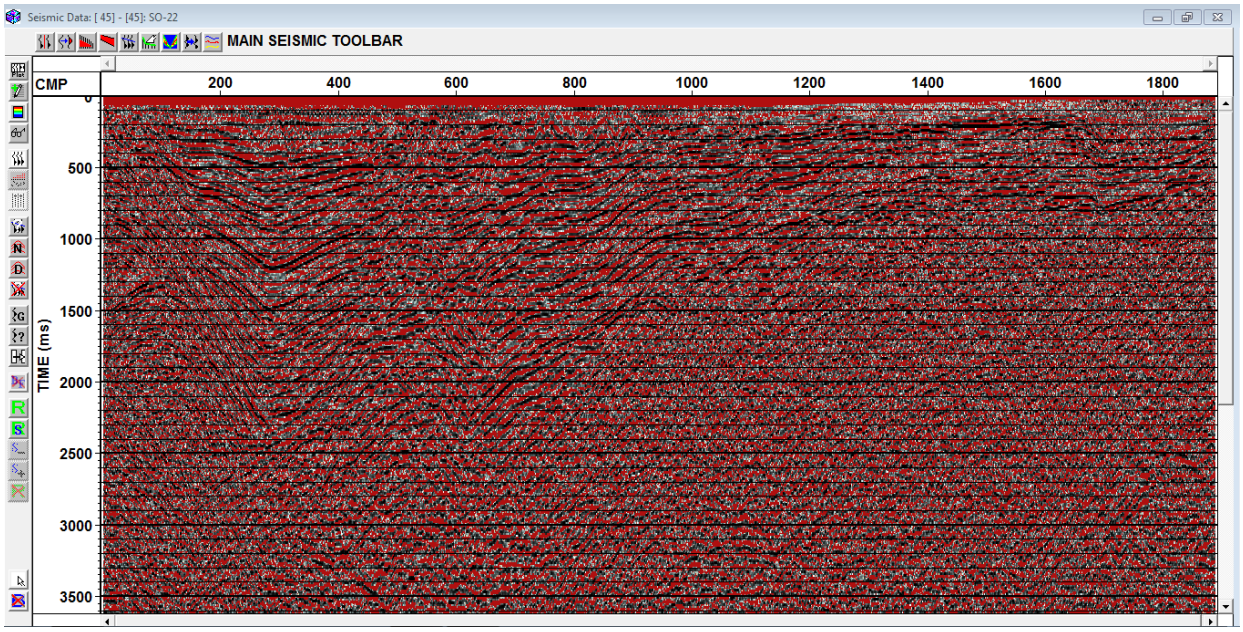

Figure 4-11: Migrated seismic section of Line SO-22.

CHAPTER FIVE

5. SEISMIC DATA INTERPRETATION

5.1. Interpretation process and method

The following is the procedures that were followed during interpretation

- Importing the SEGY data on the database of OpendeTect to observe their position on the 2D line distribution.
- Viewing of the seismic data using OpendeTect viewer. This helps to check and to see header information such as coordinates and shot points.
- Caliper, Spontaneous Potential (SP) and Gamma Ray (GR) logs are used to identify the horizons in time depth section.
- Master well logs are also used to identify the horizons lithological behaviors and their ages.
- Lithostratigraphic column of Sabisa -1 are presented on Appendix A. (Figure A-8).

The Seismic data were interpreted using borehole data from Sabisa-1 well acquired in South Omo basin. Lithological information was taken from the lithological description of Sabisa-1 well. The logs were loaded onto the vertical seismic display of seismic line SO-45 for identification of horizons. Interpretation of each seismic line was done to extract structural, Stratigraphic information as well as to determine prospective structures. Figures 5-1 and 5-2 shows the 3D view and 2D view of the intereprted seismic lines respectively.

5.2. Horizon Interpretation

Horizon interpretation was done by using master well logs of Sabisa-1 well on vertical display of lines SO-45 and SO-22. The procedure was first to identify the horizons based on the depositional ages. This is followed by creating different horizons by

manual picking. The next step is to extrapolate these horizons to the remaing lines ready for interpretation.

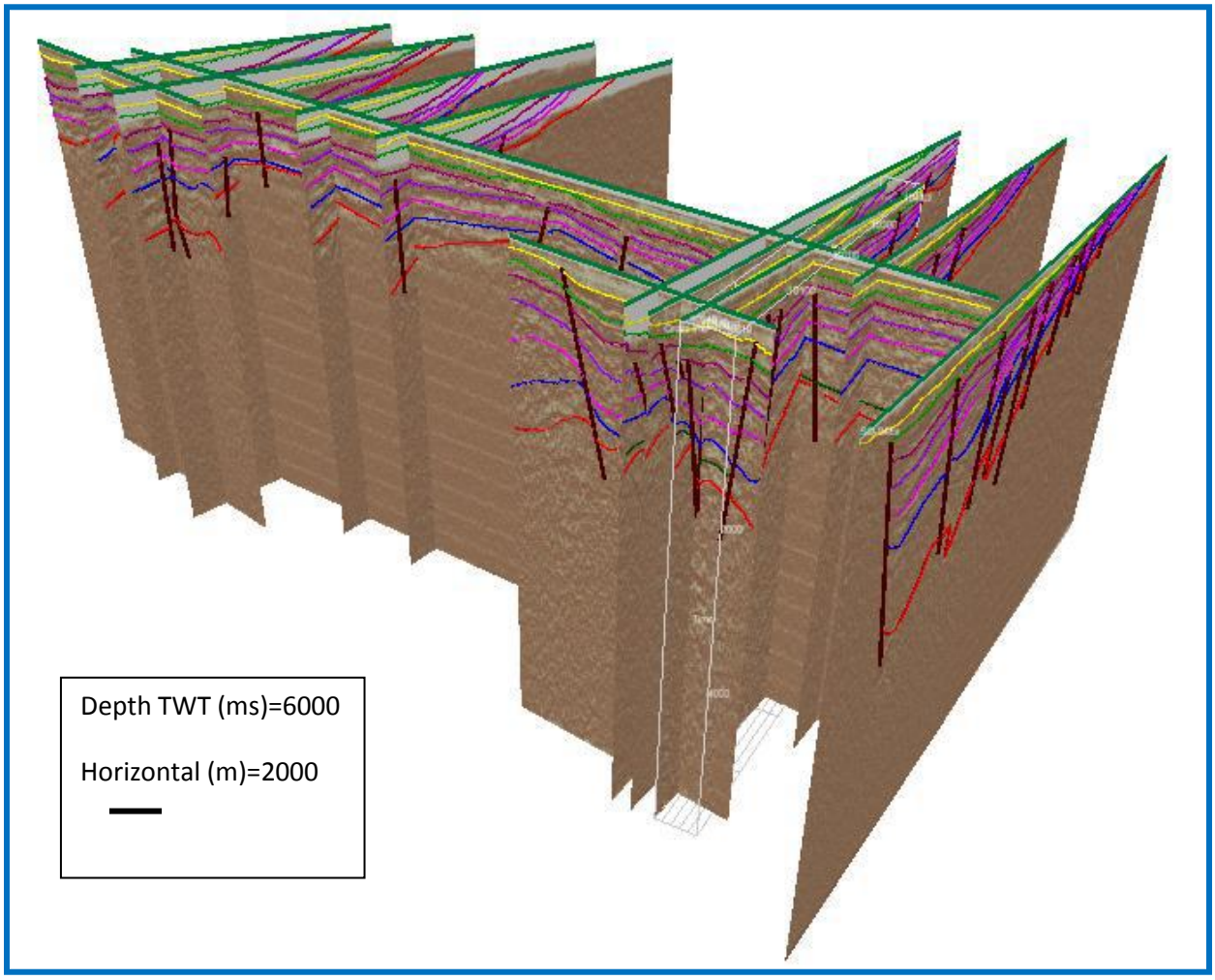

Figure 5-1: Horizon and fault Interpreted of selected lines in 3D veiw.

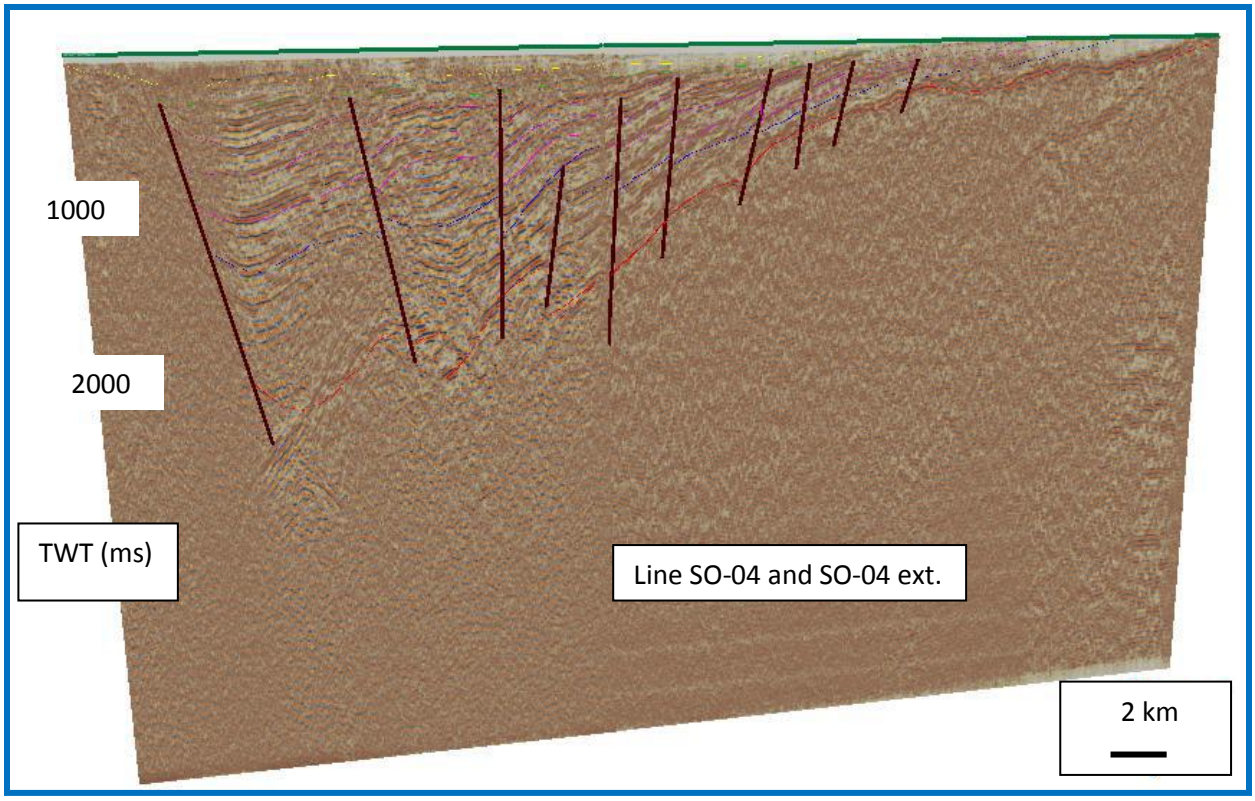

Figure 5-2: Interpreted 2D view of Seismic line SO-04 and SO-04 ext.

5.3. Fault interpretation

Fault surfaces are identified by finding termination in otherwise continuous horizons. Fault interpretation was done in the same way as horizon interpretation manually by selecting and defining major fault patterns observable on the seismic sections. Other minor faults were also interpreted.

5.4. Interpretations of Seismic Sections

The processed sections along the various lines are interpreted and shown in Figures 5-3 to 5-9. On the vertical seismic display of seismic line SO-45 eight horizons were selected based on the depositional age. The result correlates with the properties of Gamma Ray and Spontaneous Potential logs of Sabisa-1 well as shown on Figure 5 -3. The bottom reflector is Precambrian basement rocks and the six reflectors are the sedimentary sequences deposited in the given ages. In the drilled well there is 49 m thick volcanic intrusion during middle Miocene period (Tullow oil, 2012 and Davidson, 1983). Two observable faults on the seismic section have been interpreted.

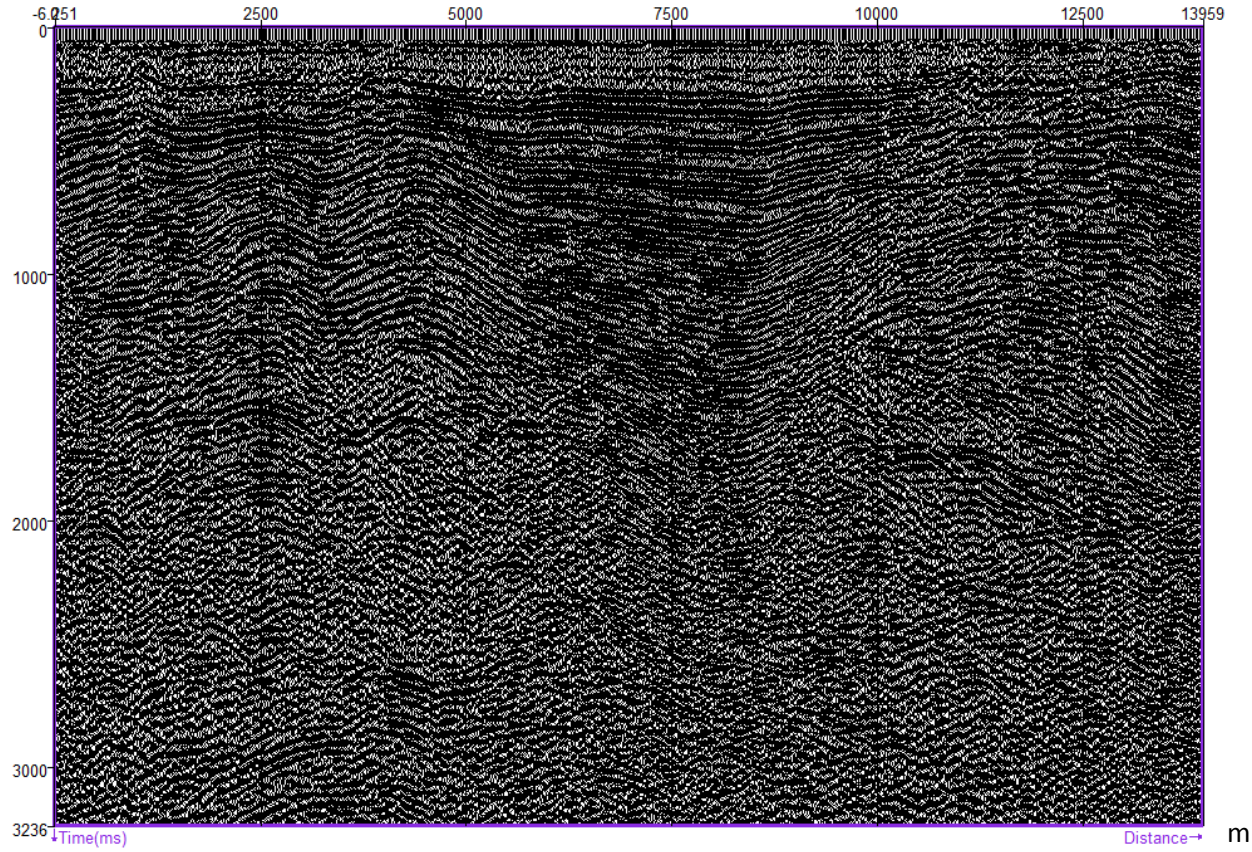

(a) Seismic line SO-45 before interpretation.

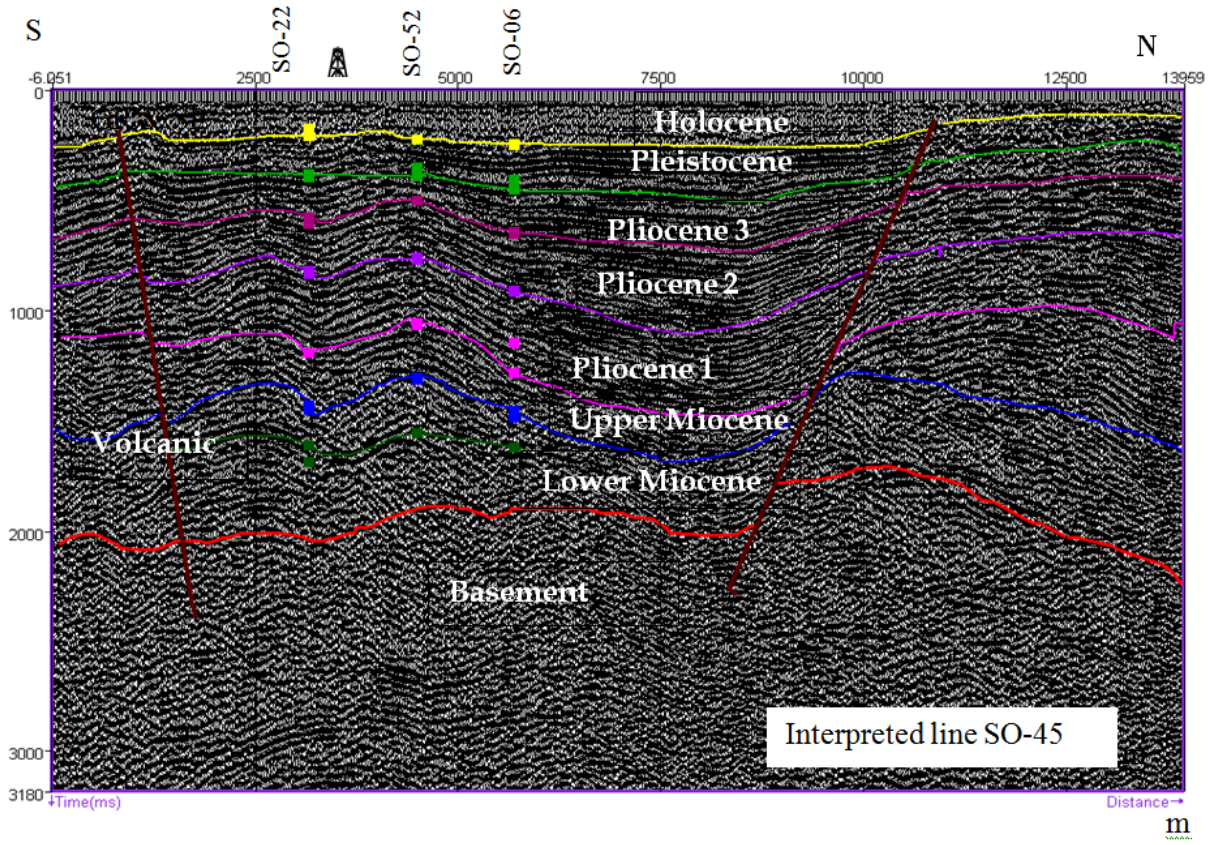

Figure 5-3: (a) before interpretation (b) Interpreted seismic section along line SO-45.

The seismic section display of line SO-22 E-W oriented line found 160m to the south of well location of Sabisa-1 (Figure 5-4). Eight horizons including the Precambrian basement and six faults are interpreted based on the projection of Sabisa-1 well. On west side of the seismic section there is a major listric type fault that shift the basement and the sedimentary sequences are pulled down and with tilted step faults in the eastern side of the seismic section.

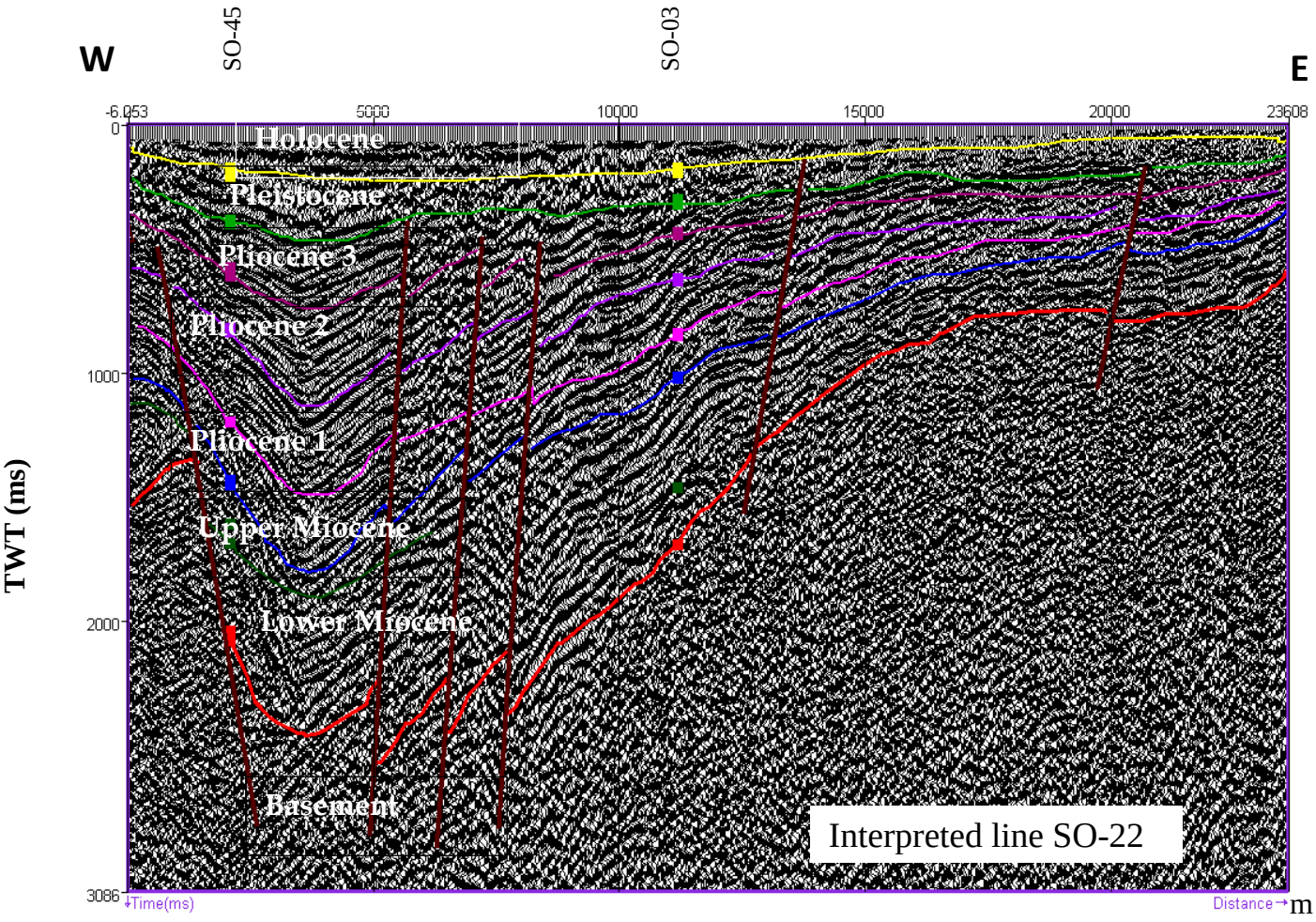

Figure 5-4: Interpreted seismic section along line SO-22.

Seismic line SO-04 is located on survey base map (Figure 1-5) at the southern edge of the Omo basin (Figure 5-5). The west tilted half graben of the South Omo interpreted by gravity (Tilahun Mammo, 2012) is clearly observed from this seismic section.

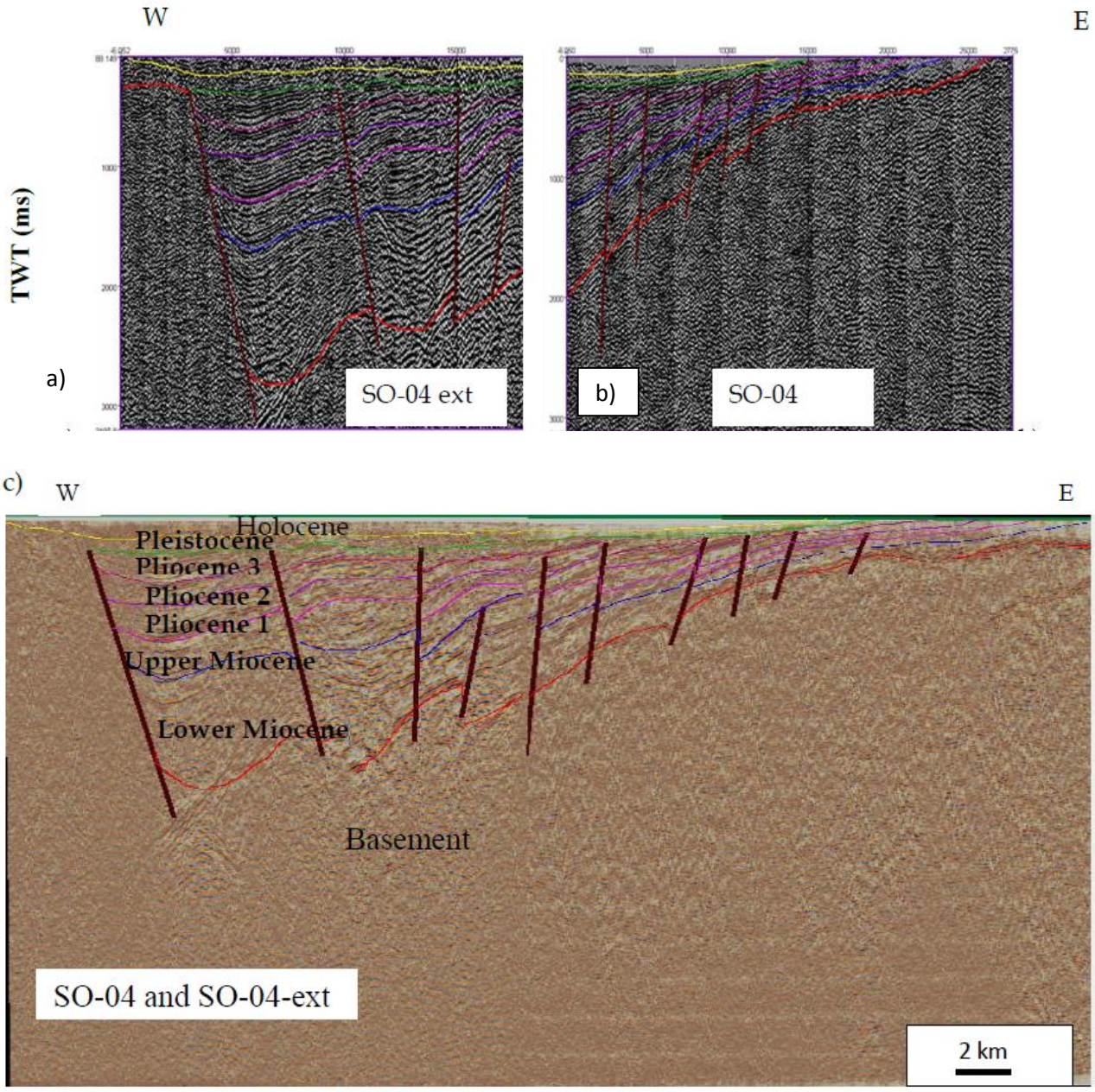

Figure 5-5: Interpreted seismic section along line (a) SO-04 ext, (b) SO-04 (c).whole section Line SO-04.

On the seismic section along line SO-20, the horizons and one flower structure with major fault and one minor fault are interpreted (Figure 5-6). The orientation of seismic line SO-20 is N-S and place that indicate deeper basin in both Magneto Telluric and gravity analysis as shown on Figures 1-2 and A-7 (Hautot, 2007 and Tilahun Mammo, 2012).

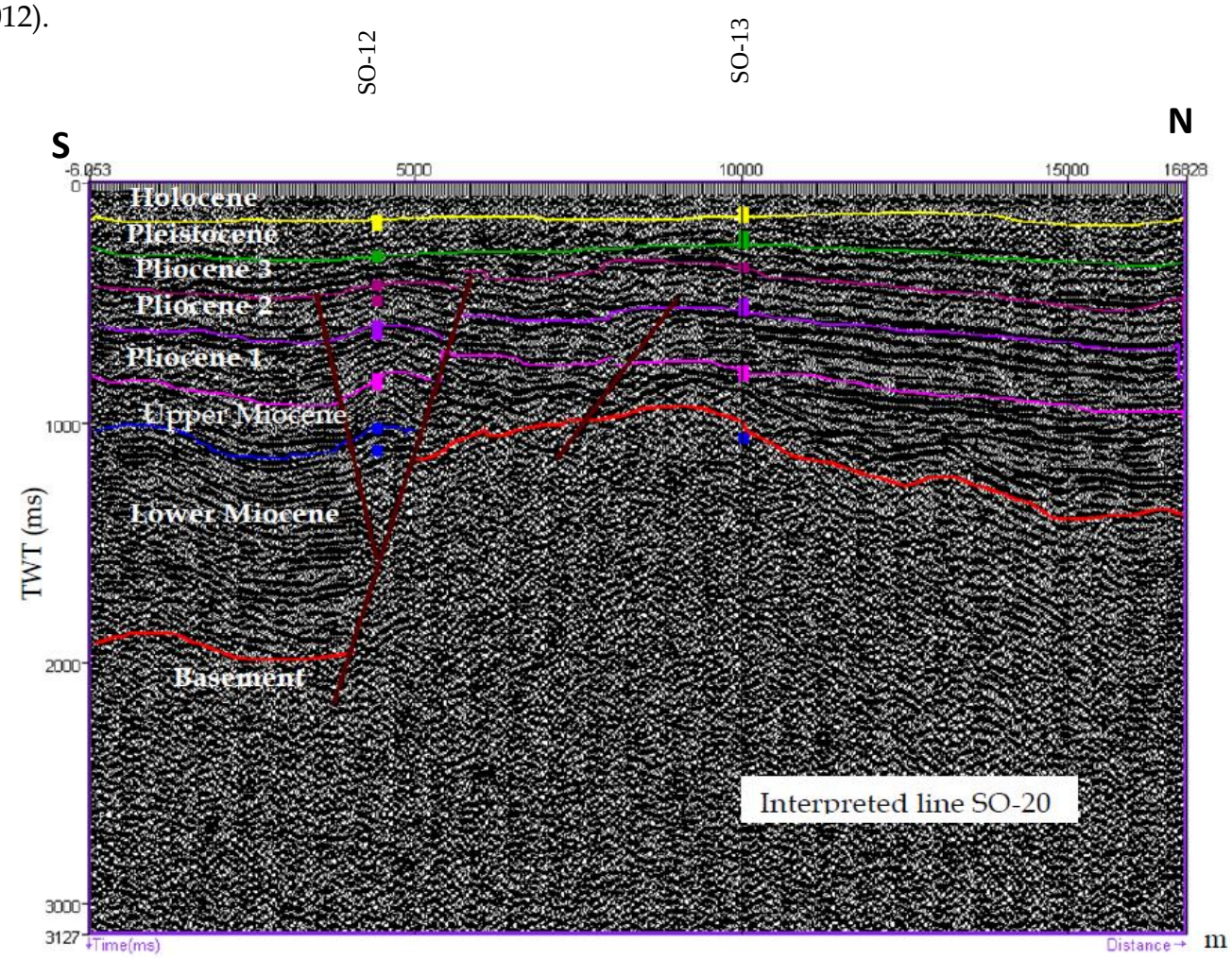

Figure 5-6: Interpreted seismic section along Line SO-20.

On section of Seismic line SO-12, four faults and seven horizons including Precambrian basement were interpreted as shown Figure 5-7. The basement rocks are shallow on eastern side of this section. The Miocene and early Pliocene age sediments are deposited on the western part of the seismic section.

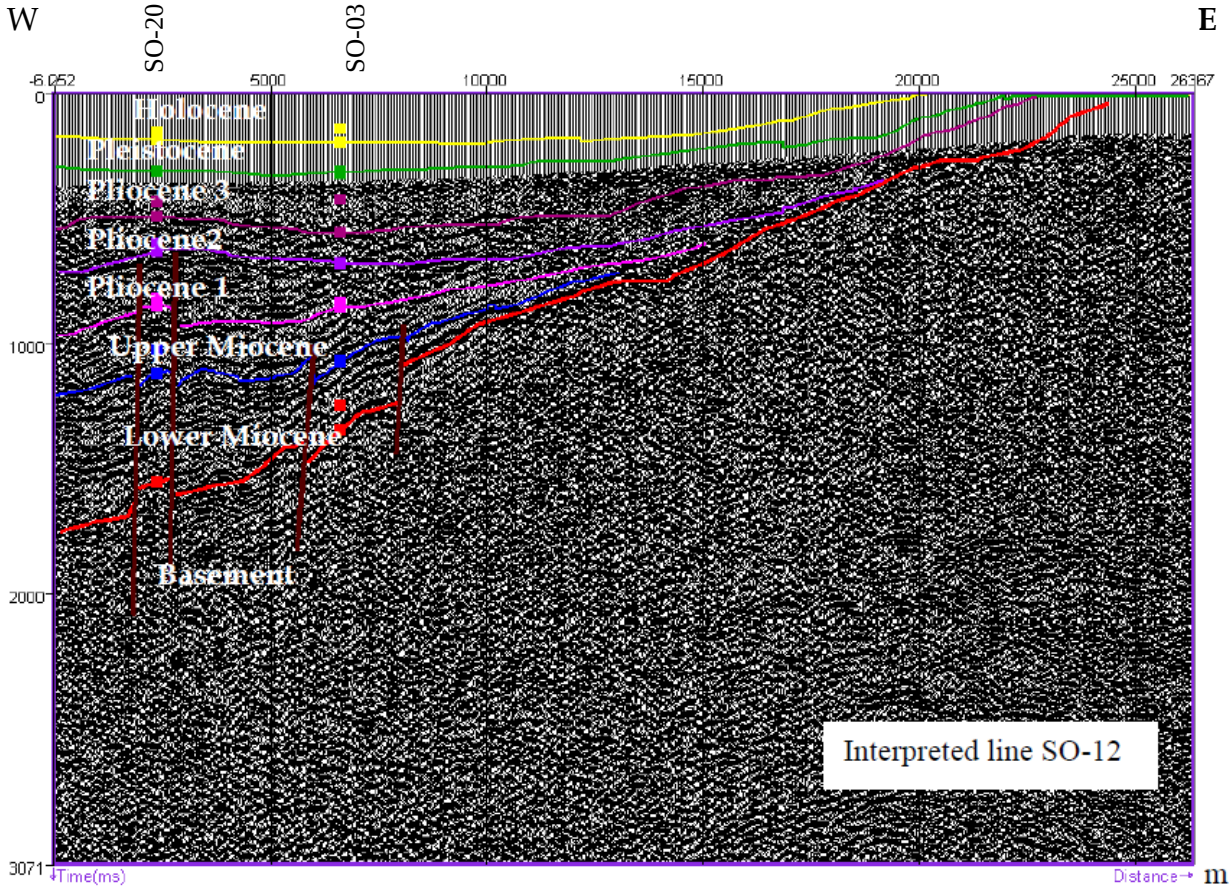

Figure 5-7: Interpreted seismic section along Line SO-12.

Seismic line SO-03 is N-S oriented line that connects all seismic lines that have E-W orientation. In the middle of this line the basement is uplifted. This result has confirmed the interpretation of gravity analysis on Figure 1-2. On Figure 5-8 seven faults are interpreted along this section. This seismic line is the longest section 56 km of all seismic lines.

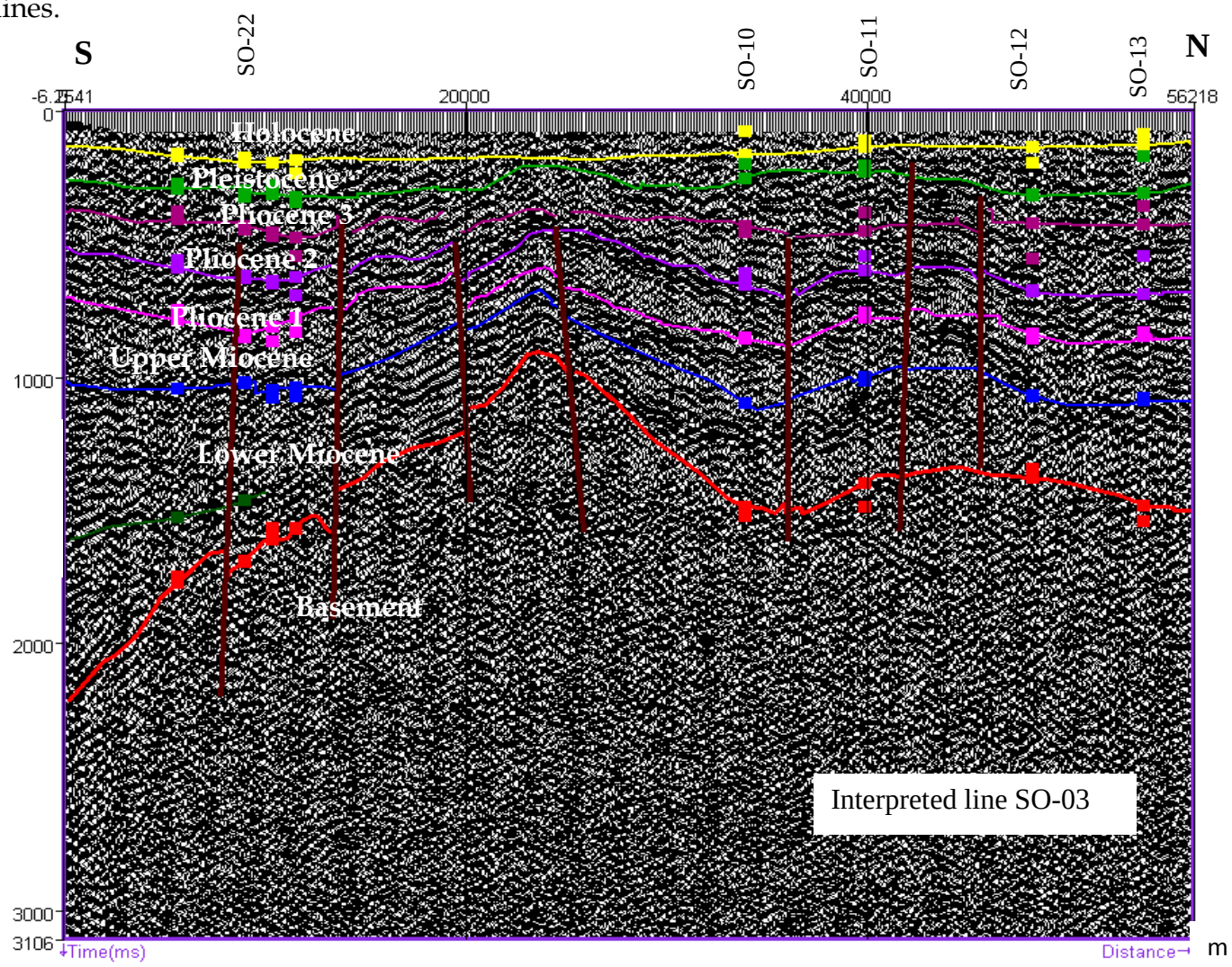

Figure 5-8: Interpreted seismic section along Line SO-03.

Of the processed lines SO-05, SO-06, SO-10, SO-11 and SO-52 are presented in the appendix A.

CHAPTER SIX

6. DISCUSSION OF THE RESULTS

6.1. Stratigraphy of the basin

From the interpreted result shown in Section Five, all E-W oriented lines indicate that South Omo basin has similar vertical seismic displays, west tilted basement and sedimentary sequences. However, on N-S oriented lines SO-45 and SO-20 the basement and the deposited sediments are undisturbed. The long line SO-03 shows that the basement is uplifted in the middle that forms southern and northern sub basins. The sedimentary sequences thin up-dip towards the eastern edge of the basin. The result of seismic interpretation confirms half graben structure that have been presented by the gravity analysis of South Omo basin (Tullow Oil Ethiopia, 2010 and Tilahun Mammo, 2012).

Lithological ages of the interpreted seismic sections of line SO-45 are assigned from the result of drilling of Sabisa-1 well. Accordingly, South Omo basin has the following lithological units: Precambrian basement rocks, Lower Miocene sediments and Volcanic flows, Upper Miocene fluvio-lacustrine sediments, the Early and Middle Pliocene sediments, Late Pliocene sediments, Pleistocene sediments and Holocene sediments.

Precambrian basement rocks

They form the base of South Omo basin and were observed on all the seismic vertical displays of the interpreted lines. Basement rocks were found to be high on both the western and the eastern sides of the basin. These rocks have shear zone along the major western fault on the seismic lines SO-22, SO-04 and SO-52 as shown in Figures 5-4, 5-5 and A-6.

Lower Miocene sediments and volcanic flows

From the well logs of Sabisa-1 these sequences of rocks overlie the Precambrian basement rocks unconformably. From the Gamma Ray response it could be possible to

suggest that these fluvial-lacustrine sediments could contain shales which are responsible for generating hydrocarbons and could, therefore, be considered as source rocks. 49m thick of volcanic flows have been reported from the drilling of Sabisa-1 as shown on Figures 5-3 and 5-4. Descriptions of cutting for volcanic are given on the well logs report.

Upper Miocene Fluvial-Lacustrine deposits

These sediments overlie the Lower Miocene with intercalation of claystone and sand/sandstone. The presence of sand in these Formations could lead as reservoir for hydrocarbons.

Early Pliocene sediments (Pliocene-1)

These sediments are lake sediments of Pliocene age represented by fluvial conglomerate and sandstone in the basin (Davidson et.al. 1973). They are one of the older Omo group sediments as shown on the seismic sections. From lithological log of Sabisa-1 well these sediments are located at depth 1170- 1725m. According to the Final well report of Tullow oil (2013) the geological description of the sediments are claystone (Dominantly moderate to light grey, moderately hard to soft, firm, earthy, silty in nature, very calcareous) and sand (white, dirty white, occasionally pink, brown, pale yellow transparent, translucent, fine to medium grained, occasionally coarse grained angular to sub angular, occasionally sub rounded, moderately sorted).

Middle Pliocene sediments (Pliocene-2)

On the lithological log of sabisa-1 these sediments are found at depth of 850-1170 m. The geological descriptions of these sediments are also claystone and sand. This could be the next deposited Omo group sediments.

Late Pliocene sediments (Pliocene-3)

At depth of 680-850 m in Sabisa-1 the deposited sediments are latest Pliocene age. From lithological log claystone and sand are intercalated.

Pleistocene sediments (Kibish Formation)

Kibish Formation named by Butzer (1971) is Pleistocene sediments. From Gamma Ray and Spontaneous Potential of well logs these sediments are found in sabisa-1 at depth of 200-400m. Thinly bedded silts and sands contain fresh water shale fish and crocodile bones which represent lacustrine and littoral faces.

Holocene sediments

Holocene sediments constitute the youngest sediment in the basin. They cover most of the South Omo basin.

6.2. Structures of the basin

6.2.1. Faults

It was confirmed from the interpreted seismic lines that the South Omo basin has a major bounding fault in the western side that dips towards the east side. This major fault is listric type in nature with no present day topographic expression on Vertical seismic display SO-52 (Figure A-6). Generally the faults are low angle normal faults on the vertical seismic displays of seismic line SO-04 near Turkana Lake (Figure 5-5). The remaining minor faults are faults occurred to accommodate the major fault. They are dipping towards the western side to the direction opposite to the major fault.

6.2.2. Syncline and anticline structures

On the vertical display seismic line SO-22 (Figure 5-4) where Sabisa-1 was drilled has syncline structure. This is also shown on the vertical seismic display of line SO-52 (Figure A-6). Interpretive result have revealed that the existence of anticline structure on seismic line SO-20.

6.2.3. Positive flower structure

Positive flower structure was observed from interpretation of Seismic line SO-20. Flower structures were interpreted in Turkana rift that are commonly associated with transfer faults (Figure 5-6).

CHAPTER SEVEN

7. CONCLUSION AND RECOMMENDATION

7.1. Conclusions

The main objective of this research was to determine the subsurface structures with the goal of identifying and delineating possible hydrocarbon prospective areas. From the sub-surface information obtained by interpretation of twelve Seismic sections, it has been confirmed that there exists a half-graben structure in South Omo basin as described by previous researchers.

Results have also confirmed that sedimentation in South Omo basin was controlled by the basin geometry and the marginal bounding fault. The fault created accommodation zone for accumulation of sediments. Sediments were thick at the western side on the N-S bounding fault and thin out towards the eastern side of the basin. Thick sediments are also observed along E-W bounding fault in seismic line 20. It seems that the sedimentary sequences have an asymmetrical cross-section.

The contact between the basement rocks and sedimentary sequences within basin was determined and was found to be at relatively shallower depth along both on the western and eastern sides of the basin. Basement reflectors were clearly distinguishable on all the vertical seismic sections of the interpreted seismic lines. Results from seismic lines SO-04, SO-22 and SO-52 have suggest that the basement rocks could be undergone shearing zone on the major listric type fault of South Omo basin.

The study has identified two major structural systems within the basin- the dominant NS oriented major bounding faults and the older NW oriented faults of the Anza rifting system. The rest of the observed faults are normal low angle faults of East African Rift system. Faults on seismic line SO-20 show positive flower with anticline structure. Folding of sedimentary sequences is observed in basin near Sabisa-1 lines SO-22, SO-52 and SO-20. Fault closures and anticlines could serve as hydrocarbon

trapping in the basin forming a possible hydrocarbon prospecting zones. There are suggestions of source rocks from Gamma logs responses and also shale outcrops in the western side Omo River (personal communication with Tilahun Mammo). The Shale could serve as seal for hydrocarbons.

7.2. Recommendations

- More seismic lines are recommended to get a clearer picture and configuration of the basin.
- It is also recommended to integrate the seismic interpretation results with findings from other geophysical results from airborne gravity, magnetic and magneto telluric.
- 3D seismic data is highly recommended to get good image of the basin.
- Flower fault structure on seismic line SO-20 could be one prospect site with further study.

REFERENCES

1. Abbate E. Bruni P. and Sagri M. (2015). Geology of Ethiopia: A review and geomorphological perspectives. *Springer Science + Business media Dordrecht*. Italy.
2. Abdella Kemal. (2013). The Effect of Climate Change on Water Resources Potential of Omo Gibe Basin, Ethiopia, MSc Thesis at Munchen University, Germany.
3. Abera Tessema. (1996). Gravity study of Omo rift system, south western Ethiopia and its regional tectonic setting. *Ethiopian Institute of Geological Survey (EIGS), Department of Geophysics,* Addis Ababa, Ethiopia: 43 pp.
4. Assefa Aklilu and Kibebew Fantu. (1999). Reconnaissance Geological study in the Omo-Chew Bahir Area, Southern Rift basins Regions, SW Ethiopia. Unpublished report. Addis Ababa, Ethiopia. 35 pp.
5. Beicip-Franlap (Petroleum Consultants). (1998). Petroleum Potential of Ethiopia. FRDE, Ministry of Mines and Energy, Petroleum Operation Department. Unpublished report. Addis Ababa, Ethiopia: 440 pp.
6. Brown F. H. (1969). Observations on the stratigraphy and radiometric age of the 'Omo Beds' lower Omo basin, southern Ethiopia, *QUATERNARIA,* **XI,** Roma: 7-14.
7. Butzer K. W. (1971). Recent history of Ethiopian delta, University of Chicago, Dept. Geog. Research paper No. 136: 184PP
8. Chorowicz J. (2005). The East African rift system. Journal of African Earth Sciences, 43:379-410. Available online at: http://www.sceincedirect.com
9. Davidson A. (1983). The Omo River Project. Reconnaissance Geology and Geochemistry of Parts of Illubabor, Kafa, Gemu Gofa and Sidamo, Ethiopia. *E.I.G.S, Bull. No.2*, Addis Ababa, Ethiopia. 89 pp.
10. Davidson A., Alemu Shiferaw, Eyob GebreLeul, Davies J. C., Moore J. M. Abera Degefu, Alemayehu W/Rufael, Muluneh Geleta. (1973). The Omo River

Project. Preliminary report of Omo River Project, Imperial Ethiopian Government. Ministry of Mines, Addis Ababa, Ethiopia. 24 pp.

11. Ebinger C. J. and Ibrahim A. (1994). Multiple episodes of rifting in Central and East Africa: A re-evaluation of gravity data. *Geol. Rundsch*. **83:** 689-702.
12. Ermyas Nigusse, Belay Wube and Samuel Aregay. (2002). Gravity and magnetic Survey in the Southern rift basins of Ethiopia. Unpublished report. Ministry of Mines, petroleum Operation Department (POD). Addis Ababa, Ethiopia. 32 PP.
13. Feibel C. S. (2011). A Geological History of the Turkana basin. *Evolution anthropology*, **20**:206-216.
14. Gadallah M.R and Fisher R. (2009). *An Introduction to Exploration Geophysics*. Springer: 274 pp.
15. Hautot S., Whaler K. and Mohammed Desissa (2007). Scientific Report on Loans 801 and 840 Magneto telluric Sub-basalt Imaging of the Omo basin, Turkana rift, South-West Ethiopia Available at: http://gef.nerc.ac.uk/documents/publications/801.pdf. Accessed on 03/16/2017.
16. Kazmin V. (1973). Geology of Ethiopia. (Explanatory note of geological map of Ethiopia 1:2,000,000). Imperial Government of Ethiopia, Ministry of Mines, Geological Survey of Ethiopia. Unpublished report. Addis Ababa, Ethiopia: 212 pp.
17. Kearey P., Brooks M. and Hill I. (2002). *An Introduction to Geophysical Exploration.* Blackwell Science publication. Oxford, Third edition: 262 pp.
18. Macgregor D. (2015). History of the development of East African Rift System: A series of interpreted maps through time. *Journal of African Earth sciences.* **101**: 232-252.
19. Mengesha Tefera, Tadiwos Chernet and Workineh Haro. (1996). Geology of Ethiopia. (Explanatory note of geological map of Ethiopia 1:2,000,000). Second Edition, Federal Democratic Republic of Ethiopia, Ministry of Mines

and Energy, *Ethiopian Institute of Geological Survey (EIGS).* Addis Ababa, Ethiopia: 212 pp.

20. Morley C. K., Lauck R., Bosher R., Stone D. M., Wigger S. T., Wescott W. A., Haun D., Basset N. and Bosworth W., (1999). Geology and geophysics of the Anza Graben. *Geoscience of Rift Systems-Evolution of East Africa*: AAPG Studies in Geology No. **44**: 67–90.
21. NOCK. (2012). National oil Corporation of Kenya (NOCK) official News letter, Energized Bulletin Issue: **002,** Kenya: 17pp.
22. POD/White Nile Joint Study Report (JSR) (2007). Unpublished report, Ministry of Mines, Petroleum and Natural Gas, Addis Ababa, Ethiopia. 70 pp.
23. PPSA. (2008) Petroleum Production Sharing Agreement. Unpublished report, Ministry of Mines, Petroleum and Natural Gas, Addis Ababa, Ethiopia.
24. Reynolds M. John. (1997). *An introduction to Applied and environmental Geophysics*, John Wiley and Sons Ltd, Chichester, England: 800 PP
25. Schuster G. T. (2010). *Basics of Seismic Imaging*. Cambridge University Press, Cambridge. 137 pp.
26. Telford W. M., Geldart L. P. and Sheriff R. E. (1990). *Applied Geophysics 2nd edition.* Cambridge University Press, Cambridge. 744 pp.
27. Tesfaye Kidane, Brown F. H. and kidney C. (2014). Magnetostratigraphy of the Fossil-Rich Shungura Formation, southwest Ethiopia, *Journal of African Earth Sciences.* **97**: 207-223.
28. Tilahun Mammo (2012). Analysis of gravity field to reconstruct the structure of Omo basin in SW Ethiopia and implications for hydrocarbon potential. *Mar. Petrol. Geol*. **29**: 104-114.
29. Tullow Oil Ethiopia B.V. (2011). Air FTG acquisition and processing report South OMO surveys, Ethiopia. Unpublished report. Ministry of Mines, Petroleum and Natural Gas, Addis Ababa, Ethiopia: 67 pp.

30. Tullow Oil Ethiopia B.V. (2012). Final Operation Report. 2D Seismic acquisition in south Omo. Unpublished report. Ministry of Mines, Petroleum and Natural Gas, Addis Ababa, Ethiopia. 87 pp.
31. Tullow Oil Ethiopia B.V. (2013). Final well Report for Sabisa-1 well South Omo basin. Unpublished repot. Ministry of Mines, Petroleum and Natural Gas, Addis Ababa, Ethiopia. 87 pp.

APPENDIX A

Interpretation of the remaining selected Seismic lines

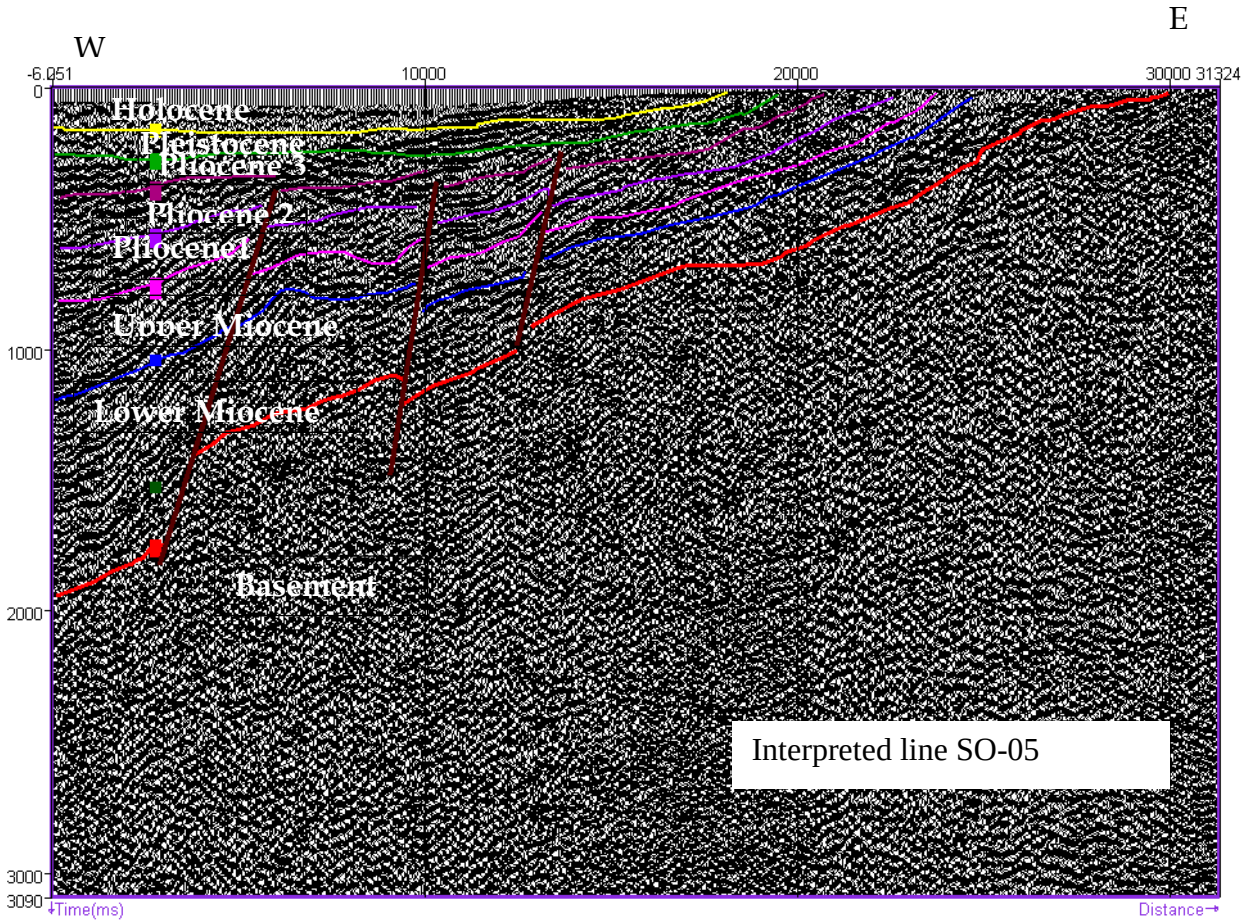

Figure A-1: Interpreted seismic section along line SO-05.

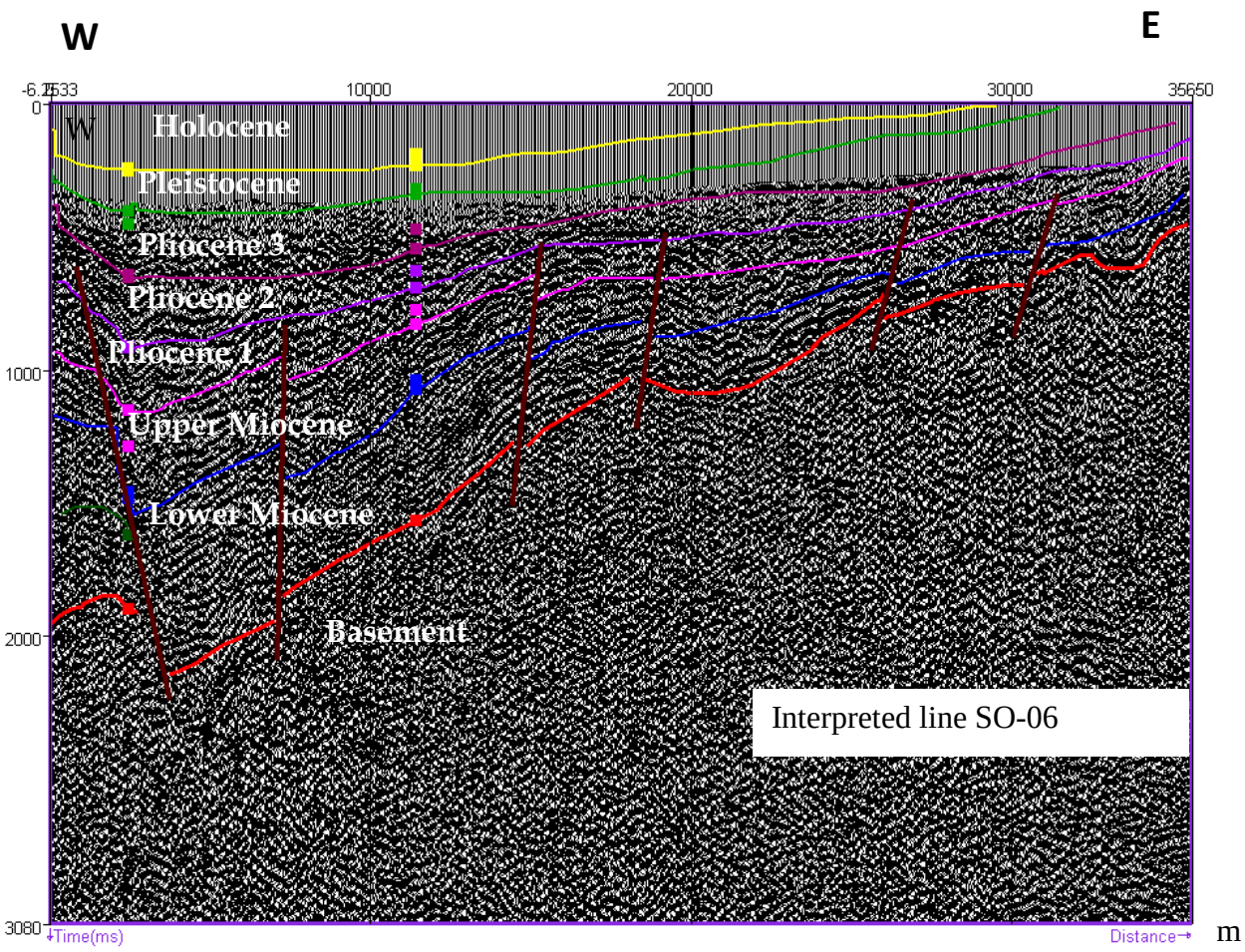

Figure A-2: Interpreted seismic section along Line SO-06.

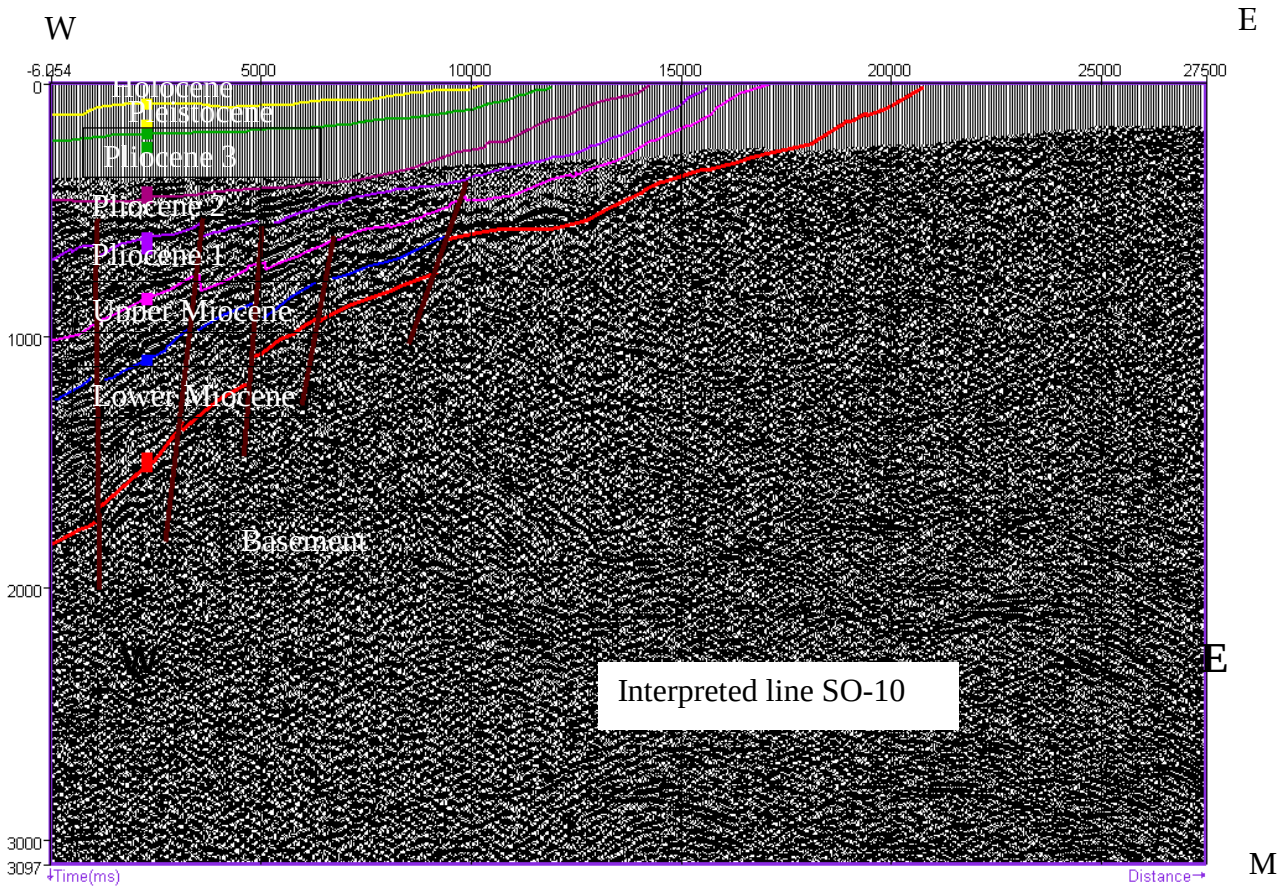

Figure A-3: Interpreted seismic section along Line SO-10.

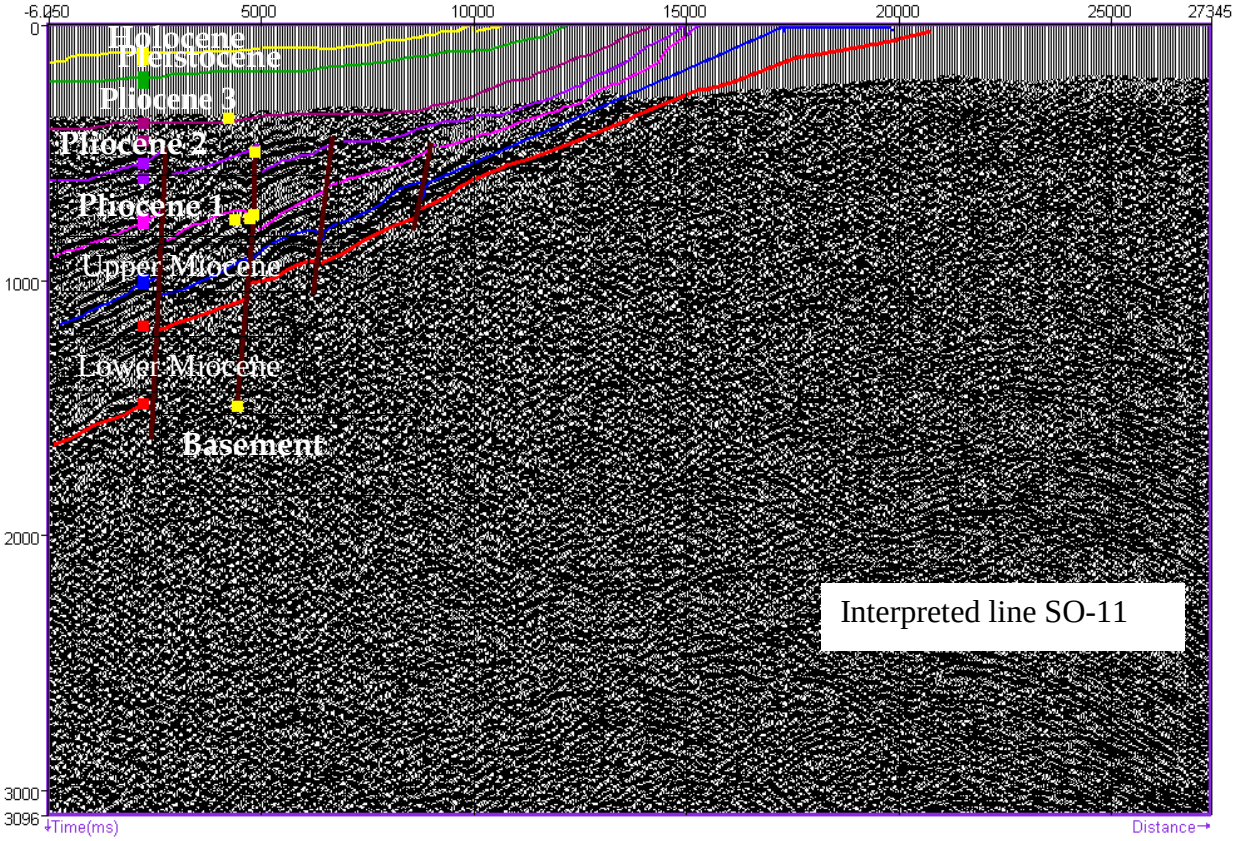

Figure A-4: Interpreted seismic section along Line SO-11.

W E

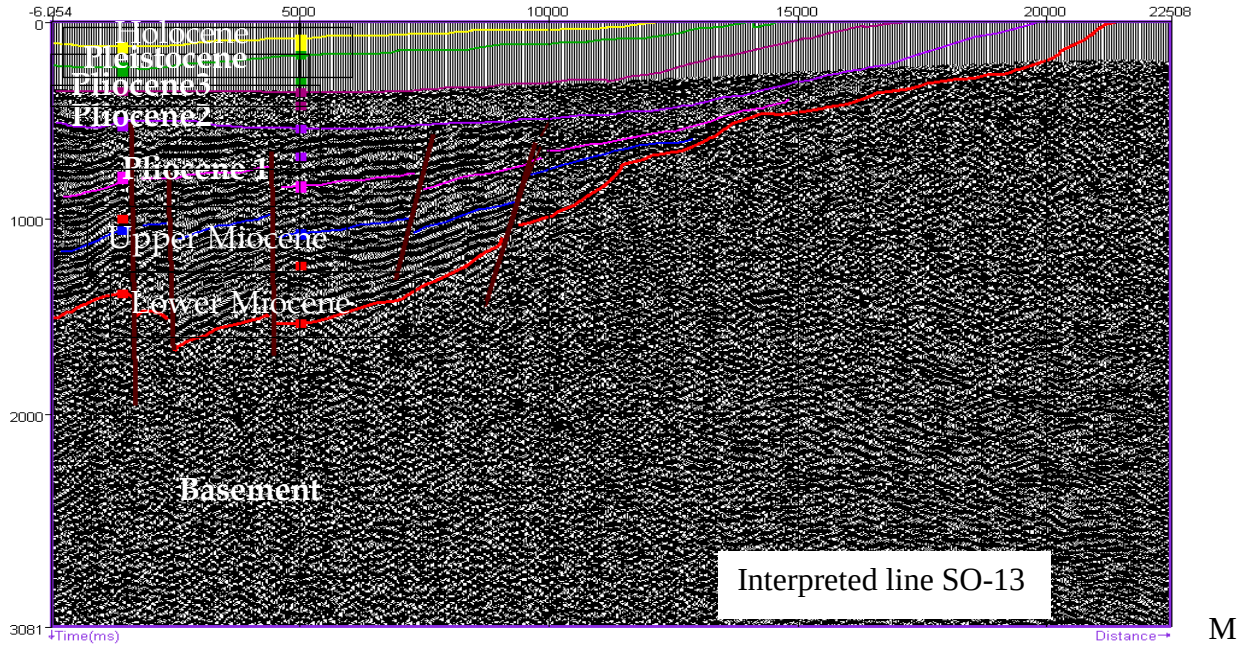

Figure A-5: Interpreted seismic section along Line SO-13.

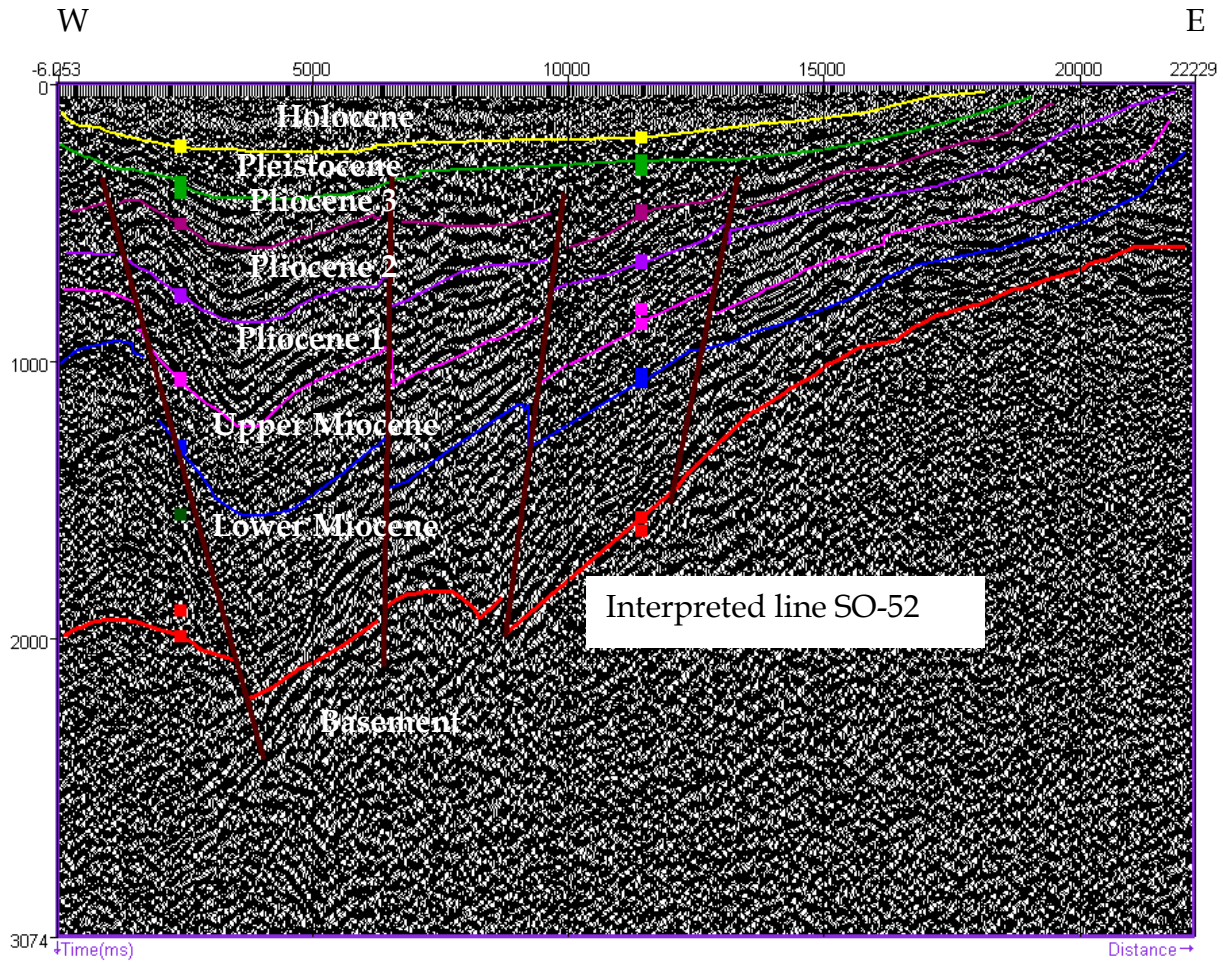

Figure A-6: Interpreted seismic section along Line SO-52.

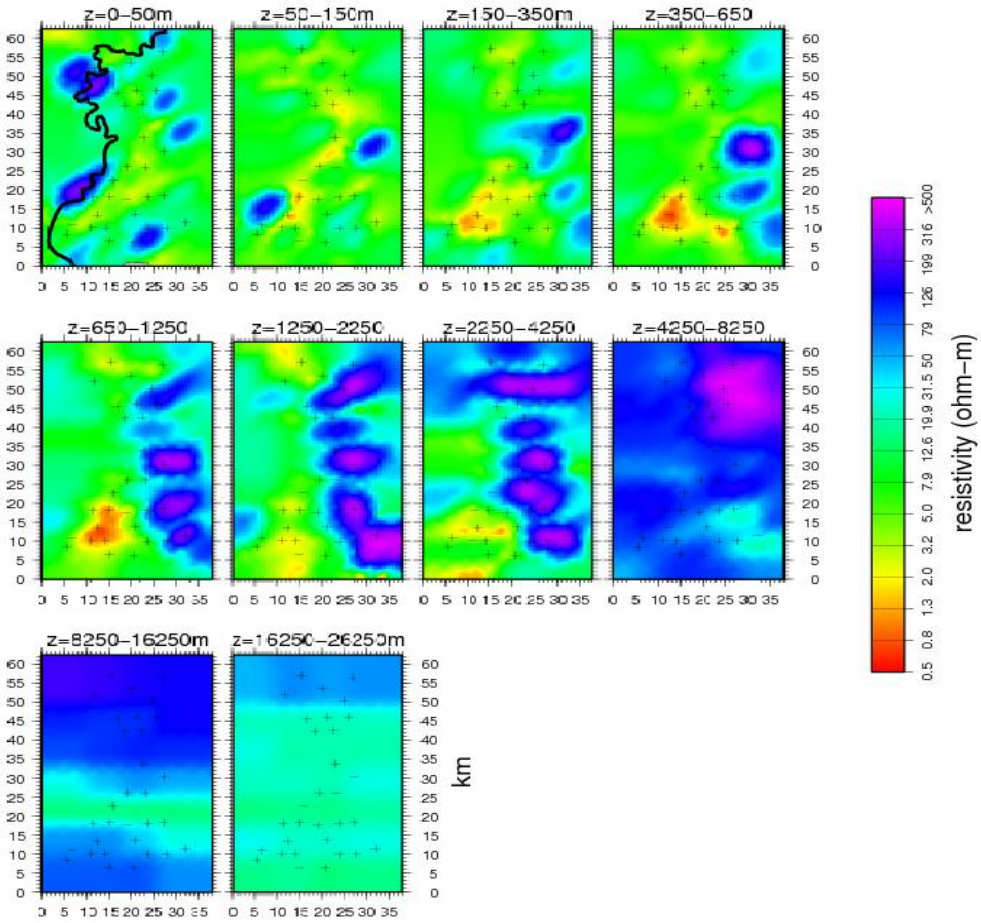

Figure A-7: MT result (after Hautot et al., 2007).

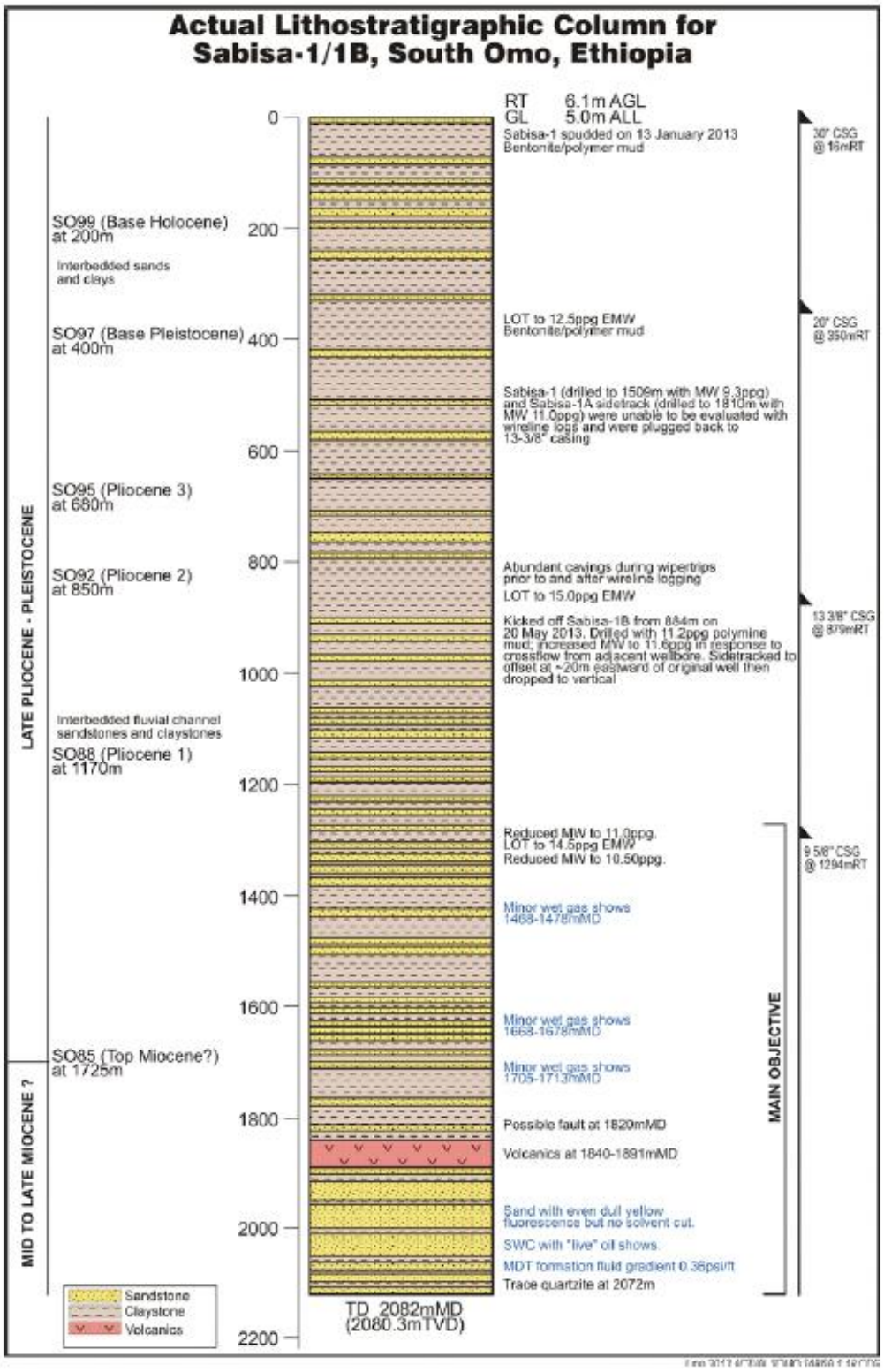

Figure A-8: Lithostratigraphic column of Sabisa 1B (after Tullow oil, 2013).